ABSTRACT

SHAH, SWAPNIL. Deriving Relations Between Connectionism and Economic Rationality in the Framework of Many-Body Physics. (Under the direction of Dr. Jon Doyle and Dr. Ki Wook Kim.)

The theory of causal entropic forces [WGF13] was introduced as an attempt to explain the principles underlying intelligent behavior from classical thermodynamic processes. It proposes that the notion of intelligence is intimately connected with maximizing future freedom of action (or the diversity of future paths the system can take) from the present time to a future horizon. In [WGF13], the authors use computer generated simulations to provide illustrations of human-like cognitive niche emergent from the action of path based entropic forces in specific simple settings. However, the theory of causal entropic forces makes no connection with the notions of rationality traditionally associated with intelligent behavior. It also fails to explain the origins of such path based forces in classical ensembles. Following the development in [Sha14], we attempt to address these issues using principles from open quantum systems theory [BP02] and the Hamiltonian theory of dynamic economics [CS76]. We show that the total entropy production is minimum starting from some initial state to a state characterized by maximum diversity of future paths.

The field of neurophysiology has produced some very detailed studies on mammalian brain activity and how it resembles the behavior of connected many-body systems in thermodynamics at their continuous phase transition point. These studies, however, are empirical in nature and lack a concrete mathematical formalism. We show how conformal symmetry, which is characteristic of the continuous phase transition point, develops in connected networks of units which maximize their future path diversity in the context of causal entropic forces. This is accomplished using the functional renormalizaton group in many-body physics and the thermodynamic Massieu function [Niv09], which is a statistical generalization of entropy production for systems evolving towards their nonequilibrium steady states.

Deriving Relations Between Connectionism and Economic Rationality in the Framework of Many-Body Physics

by
Swapnil Shah

A thesis submitted to the Graduate Faculty of
North Carolina State University
in partial fulfillment of the
requirements for the Degree of
Master of Science

Computer Engineering

Raleigh, North Carolina
2015

APPROVED BY:

Dr. Jon Doyle Co-chair of Advisory Committee	Dr. Ki Wook Kim Co-chair of Advisory Committee

Dr. Andrew Rindos

DEDICATION

To my parents,
Nitin Shah & Rupali Shah

BIOGRAPHY

Swapnil Nitin Shah was born on April 27, 1990 in Anand, Gujarat, India. He completed his schooling from Bright High School, Vadodara, India and subsequently earned his bachelors degree in Electronics and Communication Engineering from National Institute of Technology, Surat, India. Post undergraduate, he was employed with Deloitte Consulting for a year as a Business Technology Analyst. He is currently pursuing a M.S. in Computer Engineering from North Carolina State University, USA.

Swapnil has been involved in Artificial Intelligence research since his undergraduate, having published a few research articles in peer-reviewed conferences and journals. As of November 2014, he is a senior member of the Artificial General Intelligence society.

ACKNOWLEDGEMENTS

I take this opportunity to extend my sincerest gratitude to Dr. Jon Doyle for his support and trust in me and my abilities to carry out credible research. I have learnt a lot under your guidance. Working with you for the past year and a half has been a greatly enriching experience, academically and otherwise. I would also like to thank Dr. Charles Matthews for introducing me to the key concepts that led to this thesis, his immense support and encouragement during the process and the enlightening discussions we had over coffee. I will cherish our friendship forever. I am extremely fortunate to have had both of you as my mentors, guiding me through every step while being extremely patient as I progressed.

I thank Dr. Ki Wook Kim for his valuable advice during the writing of this thesis and Dr. Andrew Rindos for taking out the time from his extremely busy schedule to serve on the committee.

I would like to thank Shikhar, Bharat, Mihir, Sushmit, Nidhi, Manish, Sahil, Dhaval and Rita; these two years have been a joyous and memorable journey only because of you. Thank you Ma and Dad for believing in me, your love gave me the strength and conviction to persist through all odds and be successful; whatever I am today and whatever I will be, I owe it to you.

TABLE OF CONTENTS

LIST OF TABLES

LIST OF FIGURES

CHAPTER

1

PROLOGUE

A fundamental unresolved problem in the field of *Artificial Intelligence* (AI) is that of a rigorous formulation of intelligent or rational behavior. The most widely studied AI architectures can be broadly categorised into *computational* and *connectionist* regimes. The computational paradigm holds that the mind is a computation that arises from the brain acting as a computing machine. All AI architectures that can be represented by a Turing Machine fall into this category. Examples include symbolic logic/knowledge based agents, goal oriented agents, (expected) utility maximizing agents, etc. On the other hand, connectionist paradigm holds that mental/behavioral phenomena are emergent processes of interconnected networks of simple units. Neural Networks, Parallel Distributed Processing (PDP), etc. are known examples in this category. Although both of these categories have witnessed decades of research and breakthroughs in isolation, not much has been done to arrive at the common principles underlying both these schools of thought.

The decision theoretic approach, also called the economic approach to rationality has had great success in planning and decision making problems. It proposes that rationality can be referred to as the agent's ability to maximize a certain value function over the sequence of states it will see in its lifetime, given the probabilities of transition for states and actions. The agent receives a reward (reinforcement) for each state it sees, based on a utility function over the sample space of states, and its job is to maximize the predicted future sum of these rewards (or the value) of its action. The

decisions made using this approach are, however, completely dependent on the utility function defined over the space of states, which is a given of the problem at hand. The conflict involved here is the lack of a consensus on the global preference order of the utilities of states, which has been a subject of great discussion in economics and philosophy [Arr50].

We propose that one way of resolving this conflict is by working out a model of the world that best fits the observations, and then reverse engineering the utility function to be consistent with how the parameters of the model evolve in time. The advantage this poses is that the extremely complex problem of subjective desirability is substituted by the (debatably) less complex problem of objective consistency. On these lines, we choose the world model to best fit the physical phenomena governed by laws of many-body physics. The thesis is organized as follows:

Chapter 2 is divided into two sections. The first section introduces and extends the notion of *Causal Entropic Forces* (CEF)[WGF13]. The theory of causal entropic forces proposes a first step towards establishing a connection between maximizing the diversity of future path and intelligent behavior. We show how maximizing diversity is closely related to minimizing the total entropy production under specific assumptions. The second section presents the results from a neurophysiological study of critical brain organization and behavior and how the activity of multiple connected neurons compares with that of simple thermodynamic systems at the critical point of phase transition. Chapters 3 and 4 present a mathematical analysis of this continuous phase transition point in physical systems.

Chapter 3 is devoted to a detailed analysis of critical phenomena in many-body systems using the *Mean Field Approximation* of statistical mechanics and subsequently using the *Renormalization Group* in field theory.

Chapter 4 introduces the reader to *Quantum Field Theory* (QFT) and provides insight into the origins of the renormalization group (RG) in QFT.

Chapter 5 is divided into two sections. The first section describes an exact mapping between *Deep Neural Network* architecture and real space RG following the development in [MS14]. The second section shows how *Conformal Symmetry*, which is characteristic of RG fixed point (critical point), develops in connected networks of units which try to maximize the expected utility measure furnished by CEF. This is accomplished using the Functional Renormalization Group and the thermodynamic *Massieu Function*, which is a statistical generalization of entropy production for systems evolving towards nonequilibrium steady states (NESS).

Chapter 6 provides a summary of the key ideas developed in the thesis: the connection between decision theoretic rationality and connectionism for a specific utility function in the framework of many-body physics. This summary is followed by a brief discussion of future work.

CHAPTER

2

THERMODYNAMICS AND COGNITION

There is a large amount of literature published on connecting statistical mechanics or classical thermodynamics with algorithmic information theory (e.g. [BS50]). At the same time, the field of neurophysiology has produced some very detailed studies on mammalian brain activity which resembles the behavior of connected many-body systems in thermodynamics; at the continuous phase transition point also called the *critical point* (e.g. [Kit09]). Although well studied in their own right, there does not exist a theory which can reconcile these ideas, which appear to be disparate, but have the common goal of explaining the principles underlying intelligent behavior from physical processes alone. This chapter begins by introducing the theory of *Causal Entropic Forces* [WGF13] as an attempt to explain emergence of intelligence as a phenomenon in classical thermodynamic systems. The next subsection throws light on the limitations of the theory and attempts to connect the notion of path-based entropy maximization as purported by CEF with economic utility theory widely accepted as a theory of rational behavior. This connect is achieved using the principles from open quantum systems theory [BP02] and the Hamiltonian theory of dynamic economics [CS76]. The second part of this chapter presents the results from a neurophysiological study of critical brain organization on how the neuronal activity compares with that of simple thermodynamic systems at the critical point of phase transition. These results, even though empirical, provide a good insight into the organization of brain structure. In the remaining part of this work, we try to show how

specific arrangements might arise in a connected network of units which try to maximize the utility measure furnished by CEF using a very powerful tool from many-body physics - the *Renormalization Group*.

2.1 Causal Entropic Forces

Wissner-Gross's theory of CEF proposes a connection between thermodynamic entropy maximization over future system paths and intelligent behavior. It claims that path-based entropic forces can result in spontaneous emergence of (seemingly) intelligent behavior in physical systems without the need for explicitly specifying goals and utilities. It suggests a potentially general thermodynamic model of adaptive behavior as a nonequilibrium process in an open system.

2.1.1 Causal Entropic Forces in Classical Ensembles

The instantaneous entropic force on a macroscopic partition of the canonical ensemble is given by

$$F = T\nabla_{\mathrm{X}} S(\mathrm{X}) \tag{2.1}$$

where T is the reservoir temperature and $S(\mathrm{X})$ is the entropy associated with a macrostate X. To maximize entropy production between the present time t and a future time horizon τ, the author hypothesizes existence of generalized causal entropic forces over paths through the configuration space rather than over the instantaneous ensemble itself. The path entropy of a macrostate X with initial system state $x(0)$ is defined by

$$S_C(\mathrm{X},\tau) = -k_b \int \Pr\big(x(t)|x(0)\big)\ln\Big(\Pr\big(x(t)|x(0)\big)\Big)\mathrm{d}x(t) \tag{2.2}$$

where $\Pr\big(x(t)|x(0)\big)$ denotes the conditional probability of the system evolving through the path $x(t)$ assuming the initial system state $x(0)$, integrating over all possible paths taken by the open systems' environment during the same interval. The path based force F_C corresponding to the path based entropy Eq. (2.2), can be expressed as

$$F_C(\mathrm{X}_0,\tau) = T_C\nabla_{\mathrm{X}} S_C(\mathrm{X},\tau)\Big|\mathrm{X}_0 \tag{2.3}$$

where X_0 is the macrostate corresponding to the initial system (micro) state $x(0)$ and T_C is the causal path temperature that parametrizes the system's bias toward macrostates that maximize causal entropy.

The remaining part of the causal path entropic force derivation takes into account specific assumptions about the environment being a heat bath at temperature T_R and that the environment is coupled to only a few of the degrees of freedom of the system, called the *forced degrees of freedom*. The thermal bath rethermalizes these forced degrees of freedom with a period ϵ. Further, if one assumes the temporal dynamics of the system to be Markovian in nature (memoryless environment), the path probability $\Pr\big(x(t)|x(0)\big)$ is given by

$$\Pr\big(x(t)|x(0)\big) = \Big(\prod_{n=1}^{N-1} \Pr\big(x(t_{n+1})|x(t_n)\big)\Big)\Pr\big(x(\epsilon)|x(0)\big) \tag{2.4}$$

Using these assumptions, [WGF13] finally derives the following form of the path based entropic force (specific details not mentioned here. The reader is referred to [WGF13] for a detailed derivation)

$$F_j(\mathrm{X}_0,\tau) = -\frac{2T_C}{T_R}\int f_j(0)\cdot\Pr\big(x(t)|x(0)\big)\ln\Big(\Pr\big(x(t)|x(0)\big)\Big)\mathrm{d}x(t) \tag{2.5}$$

The effect of the above force can be seen as driving the forced degrees of freedom of the system with a temperature dependent strength T_C/T_R in an average of short term directions $f_j(0)$, weighted by the diversity $-\Pr\big(x(t)|x(0)\big)\ln\Big(\Pr\big(x(t)|x(0)\big)\Big)$, of long term paths that they make reachable. Here the path diversity is measured over all the forced and non-forced degrees of freedom of the system. If the time horizon $\tau\to\infty$, Eq. (2.5) takes the following form owing to the asymptotic equipartition property (AEP) of statistics

$$F_j(\mathrm{X}_0,\tau) \approx \frac{2T_C\cdot\bar{H}(\mathrm{X})}{T_R}\sum\nolimits_j f_j(0)\cdot\Pr\big(x(t)|x(0)\big) \tag{2.6}$$

where $\bar{H}(\mathrm{X})$ is the entropy rate of the Markov process. Eq. (2.6) is valid if the Markov chain is ergodic and stationary, which is the condition for AEP to hold.

2.1.2 Limitations of CEF

The theory of causal entropic forces leaves open two very important questions - a) The definition of causal entropic forces, in terms of actions that maximize the statistical diversity of future paths a system can take, makes no connection with concepts of knowledge and rationality traditionally associated with intelligence. b) The theory does not explain the origins of such path based forces as against those based on the instantaneous configuration of the ensemble which are widely studied in traditional statistical mechanics. The next few sections try to address these issues using principles from open quantum systems theory [BP02] and Hamiltonian theory of dynamic economics [CS76].

The construction finally arrived at is more general than the notion of entropic forces and shows how maximizing future path diversity is closely related to maximizing a particular utility measure (negative entropy production) over a sequence of actions till the system attains a steady state.

2.1.3 Causal Entropic Forces in a Quantum Universe

In non-relativistic quantum mechanics, all matter in the universe is expressed in the form of a universal *wavefunction* which associates a non-zero complex probability amplitude to every coordinate in the combined configuration space of all particles. Unlike Euclidean space, each point in this configuration space associates a value to commuting degrees of freedom of all the particles described by the theory. The time evolution of this universal wavefunction ψ is described by the *Schrodinger wave equation*

$$i\hbar\frac{\partial\psi}{\partial t} = H\psi \tag{2.7}$$

where H is the quantum Hamiltonian which is obtained by quantizing the corresponding classical Hamiltonian by replacing the Poisson bracket $\{A, B\}$ of quantities A and B in the classical Hamilton's equations of motion by the canonical commutator $[\hat{A}, \hat{B}] \equiv \hat{A}\hat{B} - \hat{B}\hat{A}$ of the respective quantum operators $\hat{A}$ and $\hat{B}$. Quantum operators $\hat{A}$ and $\hat{B}$ for which $[A, B] = 0$ are called commuting operators (also observables if they represent physically measurable quantities). If the values of all the commuting observables are not known simultaneously, one does not have a unique wavefunction describing the state. In this condition, the state can be represented by a (probability) *density operator* which describes a statistical ensemble of wavefunctions

$$\rho = \sum\nolimits_k p_k |\psi_k\rangle\langle\psi_k| \tag{2.8}$$

where we have used the Dirac bra-ket notation to describe the wavefunction and its adjoint. $|\psi_k\rangle$ denotes the k^{th} wavefunction describing the state and p_k is the corresponding probability. It can be easily shown that the density operator ρ is positive definite and can always be diagonalized in a particular eigenbasis (if expressed in a matrix form). The time evolution of the density operator ρ is then given by the statistical generalization of the Schrodinger wave equation; the *Von Neumann-Liouville* equation

$$i\hbar\frac{\partial\rho}{\partial t} = [H, \rho] \tag{2.9}$$

If the universe is separated into a system and an environment in thermal equilibrium at some temperature T, the density matrix is given by the Gibbs state of maximum entropy

$$\rho_{\text{th}} = \frac{e^{-\beta H}}{\text{Tr}\left(e^{-\beta H}\right)} \tag{2.10}$$

where $\beta \equiv 1/k_b T$ is the inverse temperature and H is now the Hamiltonian of the system in contact with the environment. In nonequilibrium dynamics, if one assumes that the environment is Markovian (memoryless) and weakly coupled to the system (Born-Markov approximation), the time evolution of the reduced system density operator (i.e., with environment degrees of freedom traced away) is given by the *Kossakowski-Lindblad equation* [BP02]

$$\frac{\partial \rho_S}{\partial t} = -\frac{i}{\hbar}\left[H_S + H_{LS}, \rho_S\right] - \frac{1}{2}\sum\nolimits_k \mu_k \left(A_k^\dagger A_k \rho_S + \rho_S A_k^\dagger A_k - 2A_k \rho_S A_k^\dagger\right) \tag{2.11}$$

where H_{LS} is the Lamb shift Hamiltonian which results in change of the quantized energy levels of the system, A_k and $A_k^\dagger$ are the k^{th} nonunitary evolution Lindblad operator and its adjoint respectively, μ_k parametrizes the dissipation rate and ρ_S is the reduced system density operator. As in the case of Langevin dynamics for classical dissipative systems, the environment (bath) thermalizes the coupled degrees of freedom of the system in the *pointer basis* (eigenbasis of measurement) after the coarse grained interaction.

2.1.3.1 Projective or Von Neumann Interactions

Assume that the reduced system density operator ρ_S is diagonal in the eigenbasis $\{|x_i\rangle\}$. The expectation value of the force F on the ensemble described by the density operator ρ_S is given by

$$\langle F \rangle = \text{Tr}\left(\frac{\partial \rho_S}{\partial t} \cdot \hat{p}\right) \tag{2.12}$$

where $\hat{p}$ is the momentum operator canonically conjugate to the observable $\hat{x}$ with the eigenbasis $\{|x_i\rangle\}$ such that $[\hat{x}, \hat{p}] = i\hbar$. Eq. (2.12) can be simplified as

$$\langle F \rangle = \sum\nolimits_i p_i \cdot \langle F_i \rangle \tag{2.13}$$

where F_i is the expectation value of the force F in the eigenstate $|x_i\rangle$. In order to simplify the formulation further, we make the specific assumptions that the Lindblad operator A_k is a projected valued measure (PVM) such that $\sum_k A_k = \mathbb{1}$, where $\mathbb{1}$ is the identity matrix, and that the dissipation rate $\mu_k = \mu$ for all components k of the ensemble. Then the non-unitary component of the force

(i.e., neglecting the Hamiltonian contribution) in an eigenstate of $\hat{x}$ is given by

$$\langle F_i \rangle = \frac{1}{2}\mu \sum\nolimits_k \left(|\langle x_i|y_k\rangle|^2 \langle y_k|\hat{p}|y_k\rangle - \langle y_k|x_i\rangle\langle x_i|\hat{p}|y_k\rangle \right) \tag{2.14}$$

where $|y_k\rangle$ is the eigenstate of the projective Lindblad operator A_k. Using the PVM condition (i.e., $\sum_k A_k = \mathbb{1}$), Eq. (2.14) can be simplified to

$$\langle F_i \rangle = \frac{1}{2}\mu \sum\nolimits_k |\langle x_i|y_k\rangle|^2 \left(\langle y_k|\hat{p}|y_k\rangle - \langle x_i|\hat{p}|x_i\rangle \right) \tag{2.15}$$

Notice the similarities between Eq. (2.15) and Eq. (2.6). The contribution of each projective operator A_k to this force on the eigenstate $|x_i\rangle$ is proportional to statistical diversity (parametrized by the Born probability $|\langle x_i|y_k\rangle|^2$) of all future paths resulting from the action of A_k on $|x_i\rangle$. Eq. (2.15) thus explains the origins of path based nonunitary (entropic) forces for projective Markovian interactions between the system and its environment.

2.1.3.2 General Interactions and Path Diversity

In general, not all interactions are projective and the Lindblad operators A_k are positive operator valued measures (POVMs which are non-projective generalizations of PVMs) such that now $\sum_k A_k^\dagger A_k = \mathbb{1}$ and unlike PVMs, A_k are not necessarily orthogonal, making it non-trivial to simplify the Eq. (2.11). For general nonequilibrium processes, the time rate of change of entropy is given by the entropy balance relation

$$\frac{\mathrm{d}S}{\mathrm{d}t} = \sigma - \overrightarrow{\nabla} \cdot \overrightarrow{J_S} \tag{2.16}$$

where σ is the total entropy production of the universe resulting from this interaction and $\overrightarrow{J_S}$ is the entropy current flowing from the system to the bath due to the heat exchange between the system and its surroundings. Formally,

$$\overrightarrow{\nabla} \cdot \overrightarrow{J_S} = -\frac{1}{T}\frac{\mathrm{d}Q}{\mathrm{d}t} \tag{2.17}$$

$$= \mathrm{Tr}\left(\mathscr{G}(\rho) \ln \rho_{\mathrm{th}} \right) \tag{2.18}$$

where $\mathrm{d}Q$ is the (infinitesimal) heat exhanged between system and its surroundings and $\mathscr{G}(\rho)$ is the Lindblad dissipator (nonunitary part of the right hand side in Linblad Equation Eq. (2.11)). The second law of thermodynamics for open systems [BP02] is then given by

$$\sigma \geq 0 \tag{2.19}$$

In this context, the diversity of future paths through the configuration space is the maximum entropy of the system that can be produced from the present state to a future time horizon. Given the reduced system density operator at present time t as $\rho_S(t)$, this notion of future path diversity is given by

$$D' = \Xi + k_b \mathrm{Tr}\big(\rho_S(t) \ln \rho_S(t)\big) \tag{2.20}$$

where $\Xi \leq 1$ is the upper bound to the attainable future system entropy (defined completely by the number of degrees of freedom for finite dimensional systems). Let the entropy at time $t = 0$ be S_0 and the current absolute entropy $S(t)$. Then maximizing path diversity Eq. (2.20) corresponds to minimizing the change in system entropy ΔS (as both Ξ and S_0 are constants). Thus

$$\max(D') \iff \min \int \dot{S} \mathrm{d}t \tag{2.21}$$

However, this notion of maximizing diversity, implication (2.21) is short-sighted, in that it does not take into account the energy cost (consumption) associated with the process. This energy cost is quantified by the first law of thermodynamics as

$$\mathrm{d}U = \mathrm{d}Q + \mathrm{d}W \tag{2.22}$$

where U is the internal energy of the system and $\mathrm{d}W$ is the (infinitesimal) useful work done by the system. In particular one is interested in minimizing the heat lost to the surroundings δQ which did not contribute to useful work. With this, the statement for maximizing path diversity D (taking into account heat dissipated) can be posed as a Lagrange optimization problem

$$\max(D) \iff \min \int \dot{S} + \lambda(t)\dot{Q} \mathrm{d}t \tag{2.23}$$

where $\lambda(t)$ is a lagrange multiplier. Using Eq. (2.17) and implication (2.23), we get using Euler-Lagrange equations,

$$\lambda(t) = -\frac{1}{T} \tag{2.24}$$

Hence

$$\max(D) \iff \min \int \dot{S} - \frac{1}{T}\dot{Q} \mathrm{d}t \tag{2.25}$$

It can be easily inferred from Eq. (2.25) that diversity D attains its maximum value when the total entropy production over the interaction $\delta\sigma$ is minimized.

2.1.4 Hamiltonian Theory of Dynamic Economics

Consider the problem of consumption-optimal growth with positive rate of time discount $\alpha > 0$. The equations of motion are given by the *Hamiltonian Theory of Dynamic Economics* [CS76] as

$$\dot{k} = \partial_q H(q,k) \tag{2.26}$$

$$\dot{q} = \partial_k H(q,k) + \alpha q \tag{2.27}$$

Here k is the vector of endowments and q is the vector of capital goods prices. H is the Hamiltonian representing the production technology which governs the time evolution of the system. The steady state at equilibrium (q^*, k^*) is the solution of

$$\partial_q H(q^*,k^*) = 0 \tag{2.28}$$

$$\partial_k H(q^*,k^*) + \alpha q^* = 0 \tag{2.29}$$

From [Bac], the optimal path to the steady state for a diffusion process is the one that maximizes the following discounted expected utility over (possibly) infinite sequence of interventions

$$S(t) = \arg\max \mathbb{E}\left[\sum_{i=1}^{\infty} U(c_i) e^{-\int_0^{\tau_i} \alpha(S(t))\mathrm{d}t}\right] \tag{2.30}$$

where c_i is the consumption at step i, $S(t)$ is the current value of quantity being consumed, $\mathbb{E}$ is the expectation taken over various c_i with a certain probability $\Pr(c_i)$ and $U(c_i)$ is the agent's utility from consumption c_i. According to [Bac], if the rate of time discount α is significantly large, the optimal policy is Markovian in nature and is characterized by a control region in which the agent takes actions, the complementary continuation region where the system evolves based on the action and a set of actions that can be taken in the control region. For the discrete time Markovian policy Eq. (2.30) reduces to the value iteration update form of the Bellman Equation

$$V(c_i)^* = \max \mathbb{E}\left[U(c_i) + V(c_{i+1})^* e^{-\int_{\tau_i}^{\tau_{i+1}} \alpha(S(t))\mathrm{d}t}\right] \tag{2.31}$$

2.1.5 Economic Utility and Entropy Production

In the open systems evolution Eq. (2.11), one can assume the characteristic dissipation rates $\mu_k = \mu$ for all components k. Then, using the standard (basis independent) form of the Lindblad dissipator [BP02] and Eq.(2.16), the time rate of change of expectation value of $\ln\left(\rho/\rho_{\mathrm{th}}\right)$ in the energy basis

$\{|\epsilon_i\rangle\}$ is given by

$$\partial_t\left\langle \ln\left(\frac{\rho}{\rho_{\text{th}}}\right)\right\rangle = \sum_i \mu\left\langle \epsilon_i\left|\sum_\omega\sum_{\alpha,\beta}\left[A_\beta(\omega)\rho A_\alpha^\dagger(\omega)\ln\left(\frac{\rho}{\rho_{\text{th}}}\right) - A_\alpha^\dagger(\omega)A_\beta(\omega)\rho\ln\left(\frac{\rho}{\rho_{\text{th}}}\right)\right]\right|\epsilon_i\right\rangle \quad (2.32)$$

where ρ_{th} is the equilibrium stationary distribution. Here we have made use of the fact that the trace remains the same for cyclic permutations of the operators, so that the unitary term disappears for the time evolution of the expectation value. Also, from the theory of open quantum systems under the Markovian approximation [BP02] we have,

$$\left[H_S, A_\alpha^\dagger(\omega)A_\beta(\omega)\right] = 0 \quad (2.33)$$

Thus Eq. (2.32) can be written as

$$\partial_t\left\langle \ln\left(\frac{\rho}{\rho_{\text{th}}}\right)\right\rangle = \mu\mathfrak{F}(t) - \mu k\cdot\left\langle \ln\left(\frac{\rho}{\rho_{\text{th}}}\right)\right\rangle, \quad (2.34)$$

where

$$\mathfrak{F}(t) = \sum_i\left\langle \epsilon_i\left|\sum_\omega\sum_{\alpha,\beta}\left[A_\beta(\omega)\rho A_\alpha^\dagger(\omega)\ln\left(\frac{\rho}{\rho_{\text{th}}}\right)\right]\right|\epsilon_i\right\rangle \quad (2.35)$$

and

$$\begin{aligned} k &= \left\langle\sum_\omega\sum_{\alpha,\beta}A_\alpha^\dagger(\omega)A_\beta(\omega)\right\rangle \\ &= \left\langle\sum_{\alpha,\beta}A_\alpha^\dagger A_\beta\right\rangle \end{aligned} \quad (2.36)$$

where we have made use of Eq. (2.33) in the second line. With the POVM condition (i.e. $\sum_{\alpha,\beta}A_\alpha^\dagger A_\beta = \mathbb{1}$), we have $k = 1$. Eq. (2.34) is a first order linear differential equation with the solution

$$\left\langle \ln\left(\frac{\rho}{\rho_{\text{th}}}\right)\right\rangle(t) = \left[\mu\int_0^t e^{\mu t'}\mathfrak{F}(t')\mathrm{d}t' + \left\langle \ln\left(\frac{\rho_0}{\rho_{\text{th}}}\right)\right\rangle\right]e^{-\mu t} \quad (2.37)$$

Using Eq. (2.16) and Eq. (2.37), the negative of entropy production ($-\delta\sigma$) is given by

$$-\delta\sigma = \left\langle \ln\left(\frac{\rho}{\rho_{\text{th}}}\right)\right\rangle(\tau_d) - \left\langle \ln\left(\frac{\rho_0}{\rho_{\text{th}}}\right)\right\rangle \quad (2.38)$$

$$= \left[-\left\langle \ln\left(\frac{\rho_0}{\rho_{\text{th}}}\right)\right\rangle\cdot\left(1-e^{-\mu\tau_d}\right) + \mu e^{-\mu\tau_d}\cdot\int_0^{\tau_d}e^{\mu t'}\mathfrak{F}(t')\mathrm{d}t'\right] \quad (2.39)$$

where τ_d is the characteristic decoherence time for the interaction. We can identify the first term on the right hand side of Eq. (2.39) with the expectation of the utility measure over the space of states in Bellman equation Eq. (2.31) as

$$-\left\langle \ln\left(\frac{\rho_0}{\rho_{\text{th}}}\right)\right\rangle \cdot \left(1-e^{-\mu\tau_d}\right) \quad \mapsto \quad \mathbb{E}\big[U(c_i)\big] \tag{2.40}$$

We therefore call the negative of entropy production Eq. (2.39), the (discounted expected) *Entropic Utility*. The term on the left of the mapping (2.40) is linearly proportional to the negative of *Kullback-Liebler divergence* (or the relative entropy) of the initial state ρ_0 from the stationary state ρ_{th} at equilibrium. KL divergence serves as a measure of how different (divergent) is the distribution ρ_0 from the stationary distribution ρ_{th}. In this sense, the expectation of utility measure U is just the negative of KL divergence and thus corresponds to the degree of informativeness in the system. Chapter 5 extends this concept to general nonequilibrium steady states by introducing *Massieu Functions* which are statistical generalizations of entropy production.

2.2 Criticality and the Brain

Self-organized criticality is an attractive model for human brain dynamics, but there has been little direct evidence for its existence in large-scale systems measured by neuroimaging. In general, critical systems (physical systems at the continuous phase transistion point) are associated with fractal or power law scaling, long-range correlations in space and time, and rapid reconfiguration in response to external inputs. In [Kit09], the authors consider two measures of phase synchronization: the phase-lock interval and the lability of global synchronization of a (brain functional) network which are explained below. Using computational simulations of two mechanistically distinct systems displaying complex dynamics, the *Ising model* and the *Kuramoto model*, they show that both synchronization metrics have power law probability distributions when these systems are in a critical state. [Kit09] further demonstrates the existence of power law scaling behavior of both pairwise and global synchronization metrics in functional magnetic resonance imaging (fMRI) and magnetoencephalographic (MEG) data recorded from normal volunteers under resting conditions. These results strongly suggest that human brain functional systems exist in an endogenous state of dynamical criticality, characterized by a greater than random probability of both prolonged periods of phase-locking and occurrence of large rapid changes in the state of global synchronization, analogous to the neuronal avalanches described in cellular systems. The next few sections follow the development prescribed in [Kit09].

2.2.1 Synchronization Metrics and Scaling

The phase lock interval (PLI) is simply the length of time that a pair of bandpass filtered neurophysiological signals, simultaneously recorded from two different MEG sensors or two different brain regions in fMRI, are in phase synchronization with each other. Thus PLI is a measure of functional coupling between an arbitrary pair of signals in the system. The lability of global synchronization (LGS) is a measure of how extensively the total number of phase locked pairs of signals in the whole system can change over time. A globally labile system will experience occasional massive coordinated changes in coupling between many of its component elements.

2.2.1.1 Phase Lock Interval

To calculate a locally time-averaged estimate of the phase difference between two time series, F_i and F_j, [Kit09] uses their wavelet coefficients derived using Hilbert transform pairs. The instantaneous complex phase vector is defined as

$$C_{ij} = \frac{W_k(F_i)^\dagger W_k(F_j)}{\left|W_k(F_i)\right|\left|W_k(F_j)\right|} \tag{2.41}$$

where W_k denotes the k^{th} scale of *Hilbert wavelet transform* and † denotes the complex conjugate. A less noisy estimate is obtained by averaging over a time using the sliding window technique as (specific details about window size in [Kit09])

$$\overline{C}_{ij}(t) = \frac{\left\langle W_k(F_i)^\dagger W_k(F_j)\right\rangle}{\sqrt{\left\langle\left|W_k(F_i)\right|^2\right\rangle\left\langle\left|W_k(F_i)\right|^2\right\rangle}} \tag{2.42}$$

The complex argument $\text{Arg}\left(\overline{C}_{ij}(t)\right)$ given by

$$\Delta\phi_{ij}(t) = \text{Arg}\left(\overline{C}_{ij}(t)\right) \tag{2.43}$$

is the local mean phase difference between the two signals F_i and F_j in the frequency interval defined by the k^{th} wavelet scale. The PLI is then defined as the period for which $\left|\Delta\phi_{ij}(t)\right|$ is smaller than some arbitrary value γ, such as $\pi/4$ which represents the midpoint between complete synchronization $\left|\Delta\phi_{ij}(t)\right| = 0$ and complete independence $\left|\Delta\phi_{ij}(t)\right| = \pi/2$.

2.2.1.2 Global Lability of Synchronization

Given estimates of the phase difference between each pair of signals in the system, it is then possible to count the number of pairs of signals that are phase-locked at any point in time. Let $N(t)$ denote the number of such pairs, then the difference in number of synchronized pairs at any two time instants separated by Δt is given by

$$\Delta^2(t, t+\Delta t) \equiv \left| N(t+\Delta t) - N(t) \right|^2 \tag{2.44}$$

Here $\Delta^2(t, t+\Delta t)$ is the lability of global synchronization. Large values of LGS indicate extensive changes in global synchronization.

2.2.2 Computational Models

Two computational models of interacting units—the Ising model and the Kuramoto model—have been used in [Kit09] to serve as a reference for comparing neurophysiological data. The specifics of these models are not mentioned here and the reader is referred to [Kit09] for the details. In this section we provide the results of simulations performed in [Kit09] for both the models

2.2.2.1 Power Law Scaling for 2D Ising Model

The computational Ising model was instantiated as a $\{96 \times 96\}$ lattice at three different temperatures: $T = 0$ (cold), $T = T_c$ (critical) and $T = 10^5$ (hot). The objective of the simulation was to estimate instantaneous phase differences between each pair of signals Eq. (2.43) and the LGS Eq. (2.44) for comparison with neurophysiological data. To provide continuous time signals in the range $[-64, 64]$ rather than binary, data was averaged over $\{8 \times 8\}$ squares resulting in 144 different time series. The simulations were initialized with spins in random configurations and iterated for 12,192 time steps. From the simulations, it was observed that the probability distributions for both PLI and LGS demonstrated power law scaling at critical temperature T_c. The results are shown in Figure 2.1

2.2.2.2 Power Law Scaling for Kuramoto Model

The 2D Ising model is one of the simplest computational models available for studying critical dynamics, which is its main advantage. However, the physical mechanism on which it is based, magnetic coupling of neighbouring spins in a ferromagnetic material, and the extreme simplicity of its components, binary spins, may seem to be implausibly related to the components and mechanisms of brain networks. The authors therefore also implemented the Kuramoto model as an alternative, independent model of critical dynamics. As against the Ising model, which is composed

of interacting binary spins, the Kuramoto model is composed of N limit-cycle oscillators each of which has its own natural frequency of oscillation and is also coupled to all the other oscillators in the system through a periodic function of their pairwise phase difference (refer [Kit09]). To generate the time series from the Kuramoto model in critical and non-critical states, the authors simulated the phase evolution of a set of 44 coupled oscillators with natural frequencies sampled from a gaussian distribution with zero mean and unit variance. Each simulation was run for 10^5 timesteps and two sets of time series were produced: one with the couplings set to the critical value $K = K_c$ and one with $K = 0$. The simulated data from the Kuramoto model shows that distributions for both

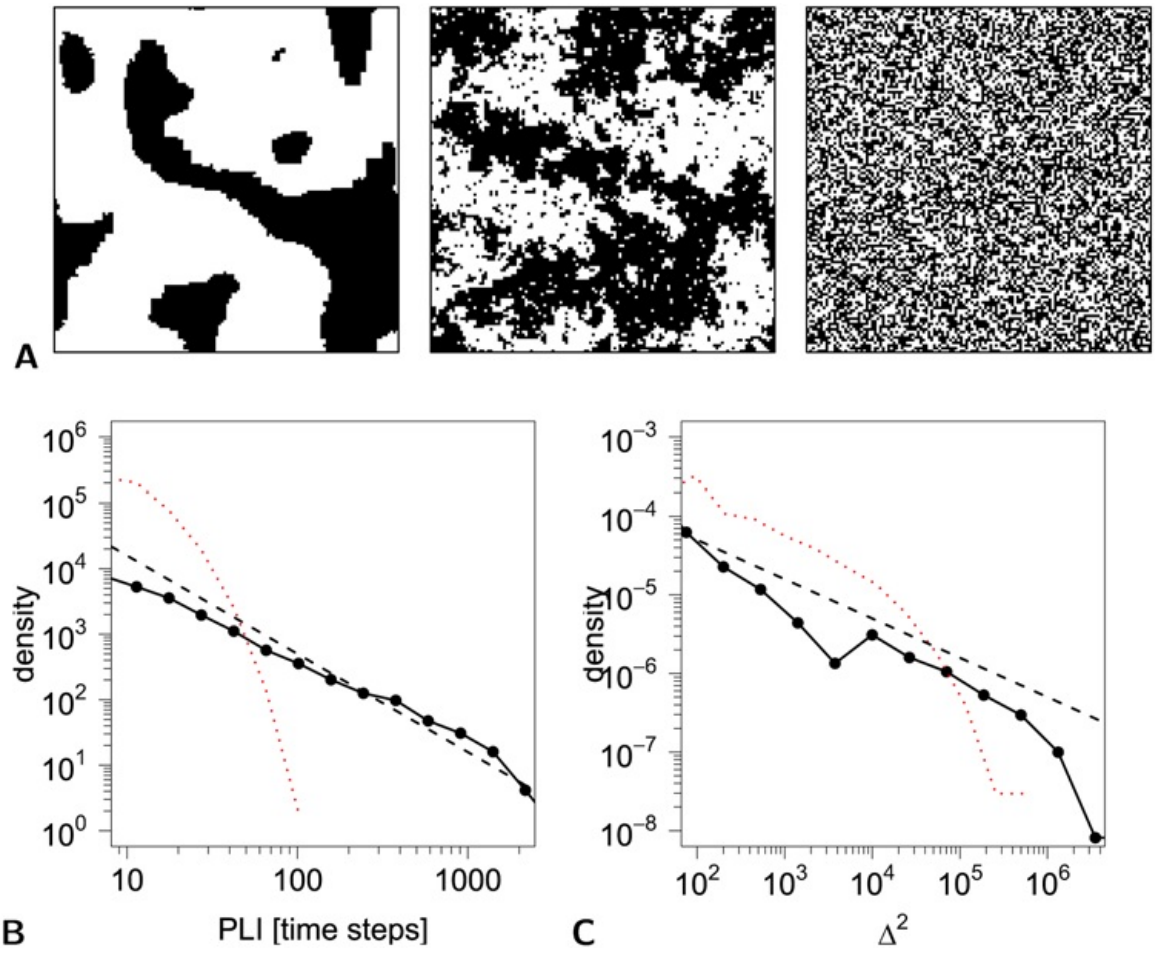

Figure 2.1 Ising model simulations of a dynamic system at critical and non-critical temperatures. Source : [Kit09] (A) Binary {128 × 128} lattices showing the configuration of spins after 2,000 timesteps at low temperature, $T = 0$ (left); critical temperature, $T = T_c$ (middle); and high temperature, $T = 10^5$ (right). (B) Probability distribution of phase lock interval (PLI) between pairs of processes at critical (black line) and at hot temperature (red line) plotted on a log-log scale.

the metrics PLI and LGS demonstrate power law scaling as expected. The results are shown in Figure 2.2

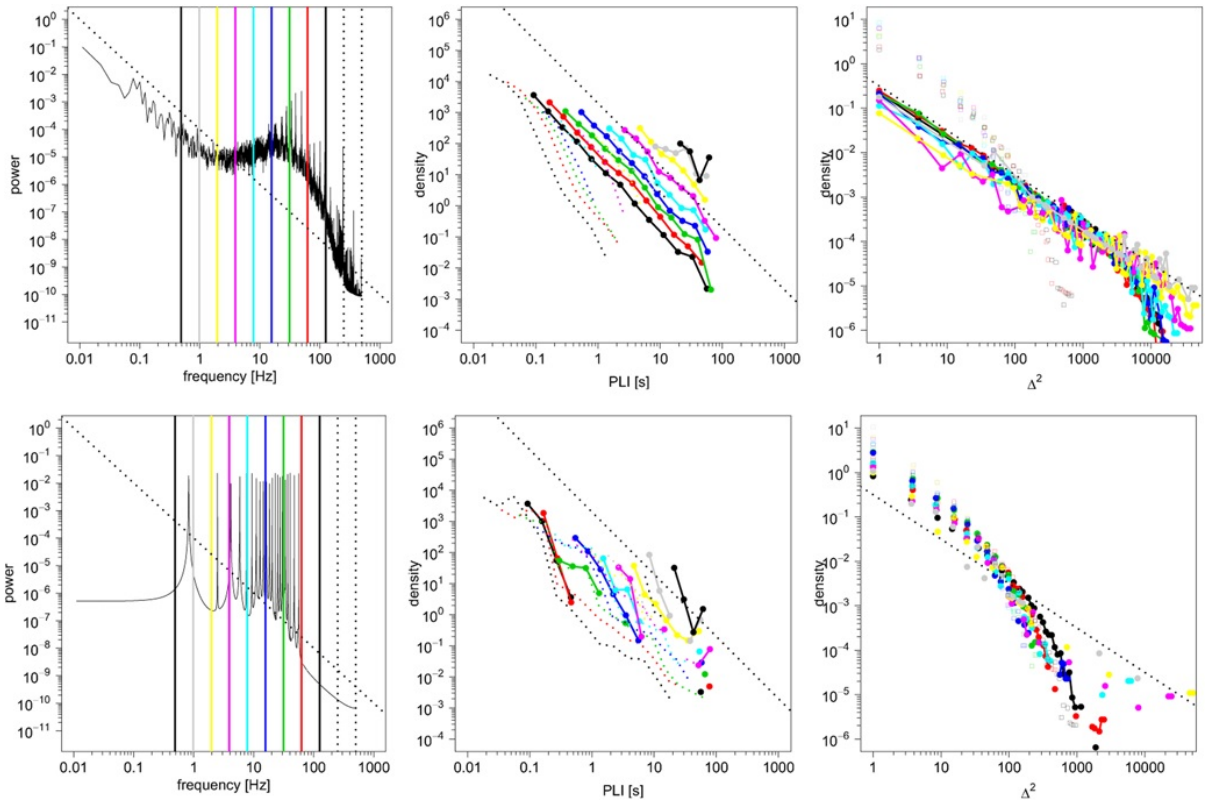

Figure 2.2 Simulated Kuramoto model data. Source : [Kit09] Top Row: Results from system at critical coupling strength K_c, Bottom Row: No coupling, i.e. free running oscillators. In all panels simulation data is denoted by solid lines (filled symbols) and the corresponding surrogate data by dotted lines. Left: Power spectrum of simulated Kuramoto model time series plotted on logarithmic axes. Center: Probability distributions for phase-lock interval PLI. Right: Probability distribution for lability of global synchronization LGS (Δ^2) is plot on logarithmic axes for each wavelet scale.

2.2.3 Functional MRI and MEG Analysis

We directly present the results for the time series analysis of fMRI and MEG data in [Kit09] obtained for human subjects. We present no details on the implementation/data acquisition as they do not impact the present work directly. Figures 2.3 and 2.4 describe the results of time series analysis on fMRI and MEG data respectively This pattern of results indicates that scaling of synchronization

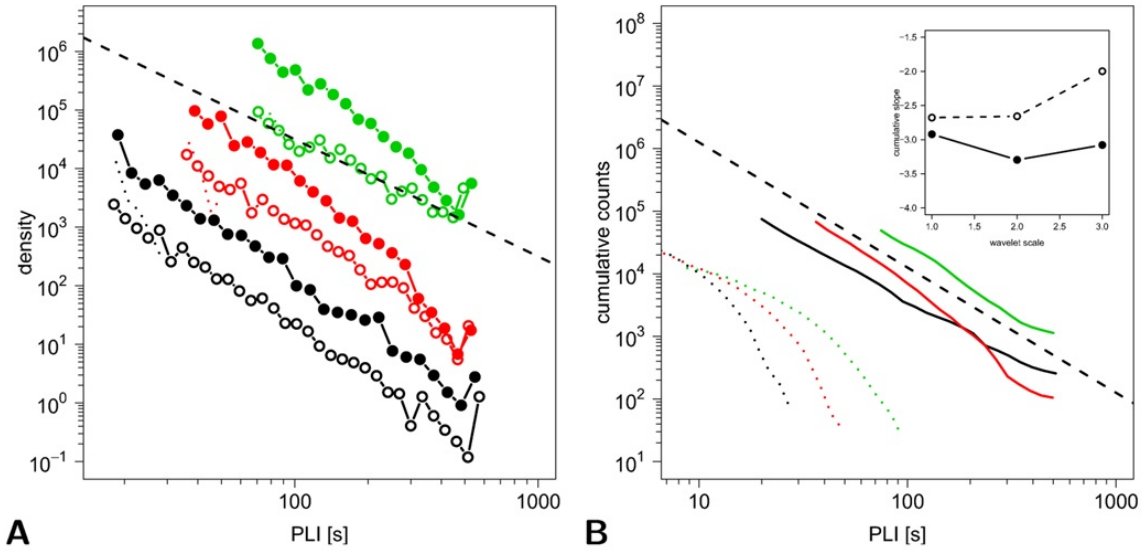

Figure 2.3 Phase-locking and global synchronization in a low frequency network measured using functional MRI. Source : [Kit09] Colors denote wavelet scales. (A) Probability distributions of phaselock interval (PLIs) are plot on logarithmic axes for all pairs of processes (filled symbols) and for all (intra-modular) pairs of processes within the same functional module (open symbols). (B) Cumulative probability distributions of phase-lock intervals are shown on logarithmic axes for all pairs of processes (solid lines) and surrogate data (dotted lines).

metrics can arise in critical systems regardless of the underlying mechanisms and that broadband criticality is clearly evident in large scale human brain networks derived from substantively different modalities of neuroimaging data. A corollary of these observations is that it is not possible to deduce the mechanism by which criticality emerges in a system simply by measuring these macroscopic behaviors. A key, unresolved question concerns the cognitive or mental significance of brain systems criticality. There is very little empirical data directly supporting the important theoretical connection between critical brain dynamics and the adaptivity or versatility of the behaviors the brain can support. In the chapters 3 and 4, we conduct a detailed mathematical study of critical phenomena in physical systems. In Chapter 5, we attempt to connect the expected Entropic Utility established in Eq. (2.39) with criticality in general connectionist architectures composed of multiple interacting units.

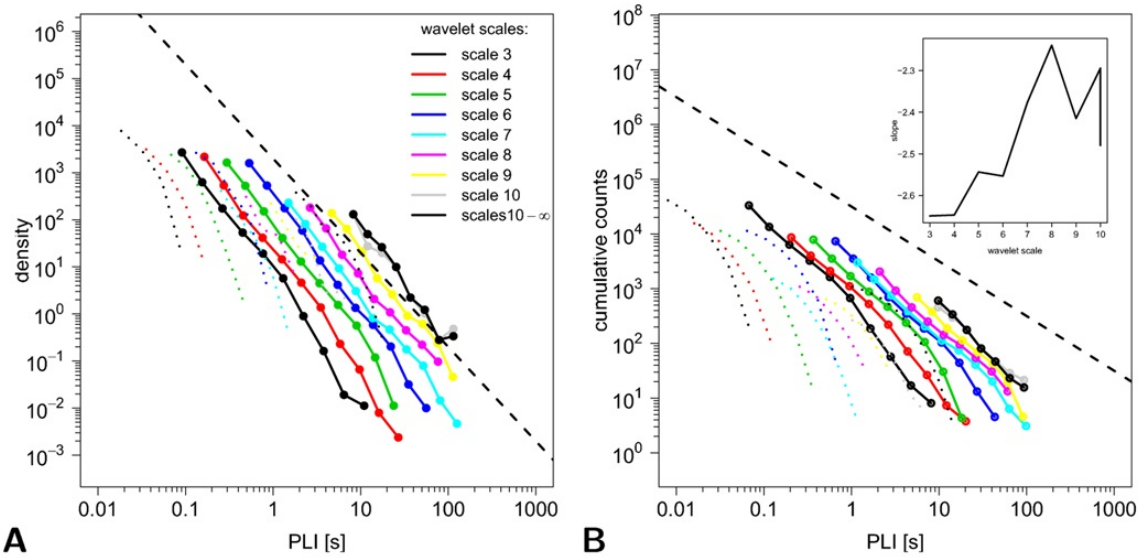

Figure 2.4 Probability distributions for phase-lock interval and lability of global synchronization in MEG data. Source : [Kit09] In all panels MEG data is denoted by solid lines (filled symbols) and the corresponding surrogate data by dotted lines. The colors encode wavelet scales. (A) Probability distribution of phase-lock intervals is plot on logarithmic axes for each wavelet scale. (B) Cumulative probability distribution of phase-lock intervals is plot on logarithmic axes for each wavelet scale.

CHAPTER

3

CRITICAL PHENOMENA

3.1 Phase Transitions

A phase transition is the transformation of a thermodynamic system from one phase or state of matter to another by transfer of heat. This term is most commonly used in the context of solid, liquid, gaseous states of matter. It can be also used to describe ferromagnetic and antiferromagnetic states in a magnetic system. However, the theory underlying phase transitions is quite general as will be seen in later chapters. Thermodynamic phase transitions have historical and modern classifications:

3.1.1 Classifications

3.1.1.1 Ehrenfest Classification

Paul Ehrenfest classified phase transitions based on the behavior of thermodynamic free energy as a function of other thermodynamic variables. Under this scheme, phase transitions were labeled by the lowest derivative of the free energy that is discontinuous at the transition. First-order phase transitions exhibit a discontinuity in the first derivative of the free energy with respect to some thermodynamic variable. The various solid/liquid/gas transitions are classified as first-order transitions because they involve a discontinuous change in density, which is the first derivative of the free energy with respect to chemical potential. Second-order phase transitions are continuous in the

first derivative (the order parameter, which is the first derivative of the free energy with respect to the external field, is continuous across the transition) but exhibit discontinuity in a second derivative of the free energy. These include the ferromagnetic phase transition in materials such as iron, where the magnetization, which is the first derivative of the free energy with respect to the applied magnetic field strength, increases continuously from zero as the temperature is lowered below the Curie temperature. The magnetic susceptibility, the second derivative of the free energy with the field, changes discontinuously. Under the Ehrenfest classification scheme, there could in principle be third, fourth, and higher-order phase transitions.

3.1.1.2 Modern Classification

Though useful, Ehrenfest's classification has been found to be an inaccurate method of classifying phase transitions, for it does not take into account the case where a derivative of free energy diverges (which is only possible in the thermodynamic limit). For instance, in the ferromagnetic transition, the heat capacity diverges to infinity. In the modern classification scheme, phase transitions are divided into two broad categories, named similarly to the Ehrenfest classes:

- **First-order phase transitions** are those that involve a latent heat. During such a transition, a system either absorbs or releases a fixed (and typically large) amount of energy per volume. During this process, the temperature of the system will stay constant as heat is added: the system is in a "mixed-phase regime" in which some parts of the system have completed the transition and others have not.
- **Second-order phase transitions** are also called continuous phase transitions. They are characterized by a divergent susceptibility, an infinite correlation length, and a power-law decay of correlations near critical point of phase transition. Examples of second-order phase transitions are the ferromagnetic transition, superconducting transition (for a Type-I superconductor the phase transition is second-order at zero external field and for a Type-II superconductor the phase transition is second-order for both normal state-mixed state and mixed state-superconducting state transitions) and the superfluid transition. Lev Landau gave the first phenomenological theory of second order phase transitions.

3.1.2 The Paramagnet-Ferromagnet Transition

The phase transition in some magnetic insulators from a paramagnetic state to a state with ferromagnetic long-range order in the absence of an external magnetic field is an example for a continuous phase transition. The thermodynamic state of the system in a magnetic field can be described

in terms of the two relevant parameters T and h. The order parameter here is the spontaneous magnetization m, which is defined in terms of the expectation value $\langle \bar{M} \rangle$ of the magnetization operator $\bar{M}$ per unit volume in the thermodynamic limit,

$$m = \lim_{h \to 0} \frac{\partial f(T,h)}{\partial h} = \lim_{h \to 0} \left[\lim_{V \to \infty} \frac{\langle \bar{M} \rangle}{V} \right], \tag{3.1}$$

The typical behavior of the spontaneous magnetization curve $m(T)$ as a function of temperature is shown in the figure 3.1 below. In the vicinity of the critical temperature T_c where m first becomes finite, the magnetization curve follows a universal power law,

$$m(T) \propto (T_c - T)^{\beta}, \quad T \leq T_c \tag{3.2}$$

where the magnetization exponent β is universal in the sense that it has the same value across a whole class of systems characterized by rather general properties such as symmetry and dimensionality. While the critical behavior described above is quite general, there are exceptions to this rule in low-dimensional systems (such as the one-dimensional Ising model), where the effect of fluctuations can prohibit spontaneous symmetry breaking at any finite temperature.

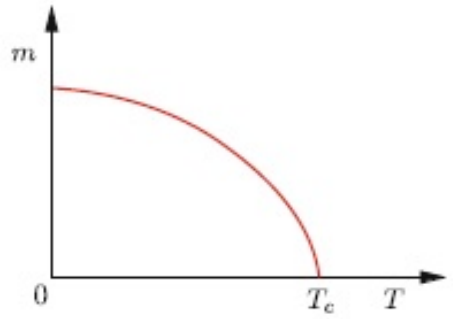

Figure 3.1 Typical behavior of the spontaneous magnetization m of a system exhibiting spontaneous ferromagnetism for temperatures T below a critical temperature T_c. Source : [Kop10]

3.2 Critical Exponents and Universality

3.2.1 Critical Exponents

As the temperature approaches the critical temperature T_c of a continuous phase transition, an increasing number of microscopic degrees of freedom are coupled to each other and effectively act as a single entity. The correlation length ξ denotes the typical length scale of the regions where the degrees of freedom are strongly coupled. For example, in the vicinity of the paramagnet-ferromagnet transition (with the temperature slightly larger than the critical temperature) microscopic spins within regions of linear size ξ tend to point in the same direction, while spins belonging to different regions whose distance is large compared with ξ remain uncorrelated. At the critical point associated with a continuous phase transition, the correlation length ξ is infinite and there are fluctuations on all length scales, so that the system is scale invariant. As a consequence, thermodynamic observables are homogeneous functions of the relevant thermodynamic variables so that they exhibit power-law behavior. The exponents which characterize the leading behavior of thermodynamic observables for $T \to T_c$ are called critical exponents. For simplicity, consider the paramagnet-ferromagnet transition. It is convenient to measure the distance from the critical point on the temperature axis in terms of the reduced temperature.

$$t = \frac{T - T_c}{T_c}, \tag{3.3}$$

Historically, one introduces the critical exponents α, β and γ to characterize the asymptotic behavior of the following observables for $t \to 0$,

Specific Heat :	$C(t) \propto \lvert t\rvert^{-\alpha}$
Spontaneous Magnetization :	$m(t) \propto (-t)^{\beta}, \quad t \leq 0,$
Magnetic Susceptibility :	$\chi \propto \lvert t\rvert^{-\gamma}$

Moreover, the shape of the critical isotherm giving the magnetic field dependence of the magnetization $m(h)$ at $T = T_c$ for a small magnetic field h defines another critical exponent δ,

Critical Isotherm :	$m(h) \propto \lvert h\rvert^{\frac{1}{\delta}} \operatorname{sgn}(h)$

The above exponents are related by the scaling hypothesis, which will be taken up in the next section. In addition to these four exponents, one usually introduces two more exponents ν and η via the behavior of the order-parameter correlation function $G(r - r')$ for large distances $r - r'$. For a magnetic phase transition with Ising symmetry, $G(r - r')$ is defined as follows. Let us denote by $\hat{m}(r)$ the operator representing the local magnetization density at space point r. By translational

invariance, the thermal average

$$m = \langle \hat{m}(r) \rangle \equiv \frac{\mathrm{Tr}\, e^{-H/T} \hat{m}(r)}{\mathrm{Tr}\, e^{-H/T}} \tag{3.4}$$

is then independent of r, so that $\delta \hat{m}(r) = \hat{m}(r) - \langle \hat{m}(r) \rangle = \hat{m}(r) - m$. The order parameter correlation function is then defined by the thermal average as

$$\begin{aligned} G(r-r') &= \langle \hat{m}(r)\hat{m}(r') \rangle - \langle \hat{m}(r) \rangle \langle \hat{m}(r') \rangle \\ &= \langle \delta \hat{m}(r) \delta \hat{m}(r') \rangle, \end{aligned} \tag{3.5}$$

which depends only on the difference $r - r'$. It is sometimes more convenient to transform $G(r-r')$ to wave vector space using the fourier transform as

$$G(k) = \int \mathrm{d}^D r \; e^{-ikr} G(r), \tag{3.6}$$

Typically, one finds that the asymptotic behavior of $G(r)$ for distances much larger compared with the correlation length ξ obeys

$$G(r) \propto \frac{e^{-\frac{|r|}{\xi}}}{\sqrt{\xi^{D-3} |r|^{D-1}}}, \quad |r| \gg \xi, \tag{3.7}$$

For $T \to T_c$, the correlation length ξ diverges with a power law,

$$\xi \propto |t|^{-\nu}, \tag{3.8}$$

where ν is called the correlation length exponent. When the system approaches the critical point, the correlation length diverges and the regime of validity of Eq. (3.7) becomes infinite. Precisely at the critical point ξ is infinite and the order-parameter correlation function decays with a power that is different from the power in the prefactor in Eq. (3.7); in D dimensions we write,

$$G(r) \propto \frac{1}{|r|^{D-2+\eta}}, \quad T = T_c, \tag{3.9}$$

To motivate the above definition of the correlation function exponent η, in the wave vector space the above equation implies for $k \to 0$,

$$G(k) \propto |k|^{-2+\eta}, \quad T = T_c, \tag{3.10}$$

It turns out that the numerical values of the critical exponents are not simply given by rational numbers as one might have expected on the basis of dimensional analysis. Moreover, the exponents are universal in the sense that entire classes of materials consisting of very different microscopic constituents can have the same exponents. As a consequence of this, a uniaxial ferromagnet and a simple fluid for example are believed to have exactly the same critical exponents. All materials can thus be divided into universality classes, which are characterized by the same critical exponents. The universality class in turn is determined by some rather general properties of a system, such as its dimensionality, the symmetry of its order parameter, or the range of the interaction.

3.2.2 The Scaling Hypothesis

It turns out that under quite general conditions, only two of the six exponents α, β, γ, δ, ν, and η are independent, so that we can obtain the thermodynamic exponents α, β, γ and δ from the exponents ν and η related to the scaling of the correlation function using so-called scaling relations. The latter follow from the scaling behavior of the free energy $f(t,h)$ and the order-parameter correlation function in the vicinity of a continuous phase transition. The scaling relations can be obtained microscopically with the help of the renormalization group. Historically, the scaling forms of the free energy (Widom 1965) and of the correlation function (Kadanoff 1966) were formulated as a hypotheses before the renormalization group was invented. In the vicinity of a continuous phase transition, we expect that $f(t,h)$ can be decomposed into a singular and a regular part,

$$f(t,h) = f_{\text{sing}}(t,h) + f_{\text{reg}}(t,h) \tag{3.11}$$

where t is given by Eq. (3.3) and h is the intensity of the external magnetic field. Sufficiently close to the critical point, the singular part $f_{\text{sing}}(t,h)$ is assumed to be determined by power laws characteristic of a given critical point. According to the scaling hypothesis for the free energy, its singular part satisfies the following generalized homogeneity relation,

$$f_{\text{sing}}(t,h) = b^{-D} f_{\text{sing}}(b_t^y t, b_h^y h) \tag{3.12}$$

where b is arbitrary scale factor and the exponents y_t and y_h are characteristic for a given universality class. It is now easy to show that with this assumption the four thermodynamic exponents α, β, γ and δ can all be expressed in terms of y_t, y_h and the dimensionality D of the system. Then, using some mathematical intuition, one can establish the following relations between the critical exponents as

described in [Kop10],

$$\alpha = 2-D\nu \tag{3.13}$$
$$\beta = \frac{\nu}{2}(D-2+\eta) \tag{3.14}$$
$$\gamma = \nu(2-\eta) \tag{3.15}$$
$$\delta = \frac{D+2-\eta}{D-2+\eta} \tag{3.16}$$

If one considers not only static but also dynamic (i.e., time-dependent) phenomena in the vicinity of a critical point, one observes that temporal correlations of the order parameter decay more and more slowly as one approaches the critical point, a phenomenon which is called *critical slowing down*. The typical decay time of temporal order-parameter fluctuations is called the correlation time τ_c. One usually observes that in the vicinity of a critical point, τ_c diverges as a power law

$$\tau_c \propto \xi^z \propto |t|^{-\nu z}, \tag{3.17}$$

where z is called the dynamic exponent.

3.3 Mean Field Theory

Before embarking onto more complex theories, in this section we describe a less sophisticated method of dealing with this problem, namely the mean-field approximation. Within the mean-field approximation, fluctuations of the order parameter are completely neglected and the interactions between different degrees of freedom are taken into account in some simple average way. This method is, however, very general and can also be used to study quantum mechanical many-body systems. For our purpose it is sufficient to introduce this method using the nearest-neighbor Ising model in D dimensions as an example. The Ising model is defined in terms of the following classical Hamiltonian,

$$H = -\frac{1}{2}\sum_{ij=1}^{N} J_{ij}\, s_i s_j - h\sum_{i=1}^{N} s_i \tag{3.18}$$

Here i and j label the sites r_i and r_j of a D-dimensional hypercubic lattice with N sites, the variables $s_i = \pm 1$ correspond to the two possible states of the z-components of spins localized at the lattice sites, J_{ij} denote the interaction between spins localized at sites r_i and r_j, and h is the external magnetic field in the z-direction. The above model is called classical because it does not involve any noncommuting operators. It is often sufficient to assume that the J_{ij} are non-zero only if the sites r_i and r_j are nearest neighbors on the lattice. Denoting by J, the uniform non-zero value of J_{ij} for

nearest neighbors, we obtain from Eq. (3.18) the nearest neighbor Ising model

$$H = -J \sum_{\langle i\, j\rangle} s_i s_j - h \sum_{i=1}^{N} s_i \tag{3.19}$$

Here $\langle i\, j\rangle$ denotes the summation over all distinct pairs of nearest neighbors. In order to obtain thermodynamic observables, we have to calculate the partition function,

$$Z(t,h) = \sum_{s_i} e^{-\beta H} \equiv \sum_{s_1=\pm 1} \sum_{s_2=\pm 1} \cdots \sum_{s_N=\pm 1} \exp\Big[\beta J \sum_{\langle i\, j\rangle} s_i s_j + \beta h \sum_i s_i\Big], \tag{3.20}$$

where β is the inverse temperature. One can analytically derive the summation Eq. (3.20) in 1 or 2 dimensions. For $D = 3$, there are no closed form solutions available and one has to rely on approximations, the simplest method being the *Mean Field Approximation*.

3.3.1 Landau Function and Free Energy

Mean-field theory is based on the assumption that the fluctuations around the average value of the order parameter are so small that they can be neglected. The average magnetization of the system is given by

$$m = \langle s_i \rangle \equiv \frac{\sum_{s_j} e^{-H/T} s_j}{\sum_{s_j} e^{-H/T}}, \tag{3.21}$$

where we have used the fact that by translational invariance, the thermal expectation values $\langle s_i \rangle$ are independent of the site label i. Writing $s_i = m + \delta s_i$ with the fluctuation $\delta s_i = s_i - m$, we have

$$s_i s_j = m^2 + m(\delta s_i + \delta s_j) + \delta s_i \delta s_j = -m^2 + m(s_i + s_j) + \delta s_i \delta s_j \tag{3.22}$$

We now assume that the fluctuations are small so that the last term can be neglected. The original Hamiltonian is then replaced by the mean field Hamiltonian

$$\begin{aligned} H_{\rm MF} &= \frac{m^2}{2} \sum_{i\, j} J_{i\, j} - \sum_i \Big(h + \sum_j J_{i\, j} m \Big) s_i \\ &= N \frac{z J}{2} m^2 - \sum_i (h + z J m) s_i, \end{aligned} \tag{3.23}$$

for nearest neighbor interactions and $z = 2D$ is the number of nearest neighbors (coordination number) of a given site of a D dimensional hypercubic lattice. As the spins in the mean-field Hamiltonian are decoupled, the partition function factorizes into a product of N independent terms

which are just the partition functions of single spins in an effective magnetic field $h_{\text{eff}} = h + z\,J\,m$,

$$\begin{aligned} Z_{\text{MF}}(T,h) &= e^{\frac{-\beta N z J m^2}{2}} \sum_{s_i} e^{\beta(h+z\,J\,m)\sum_i s_i} \\ &= e^{\frac{-\beta N z J m^2}{2}} \Big[2\cosh[\beta(h+z\,J\,m)]\Big]^N \end{aligned} \tag{3.24}$$

Writing this as

$$Z_{\text{MF}} = e^{-\beta N \mathscr{L}_{\text{MF}}(T,h;m)}, \tag{3.25}$$

we obtain in the mean field setting,

$$\mathscr{L}_{\text{MF}}(T,h;m) = \frac{z\,J}{2} m^2 - T \ln\Big[2\cosh[\beta(h+z\,J\,m)]\Big] \tag{3.26}$$

The function $\mathscr{L}_{\text{MF}}(T,h;m)$ is an example for a Landau function, which describes the probability distribution of the order parameter: the probability density of observing the order parameter to have the value m is proportional to $\exp[-\beta N \mathscr{L}_{\text{MF}}]$. The so-far unspecified parameter m is now determined from the condition that the physical value m_0 of the order parameter maximizes its probability distribution, corresponding to the minimum of the Landau function. From Eq. (3.26) we then find that the magnetization m_0 in mean field approximation satisfies the self-consistency condition

$$m_0 = \tanh[\beta(h + z\,J\,m_0)] \tag{3.27}$$

which defines m_0 as a function of T and h. The mean field result for the free energy per site is thus,

$$f_{\text{MF}} = \mathscr{L}_{\text{MF}}(T,h;m_0) \tag{3.28}$$

It can be easily seen that for $h \neq 0$ the global minimum of $\mathscr{L}_{\text{MF}}(T,h;m_0)$ always occurs at a finite $m_0 \neq 0$. On the other hand if $h = 0$, the existence of nontrivial solutions with $m_0 \neq 0$ depends on the temperature. In the low-temperature regime $T < z\,J$ there are two nontrivial solutions with $m_0 \neq 0$, while at high temperatures $T > z\,J$ the self-consistency equation Eq. (3.27) has only the trivial solution $m_0 = 0$. In D dimensions the mean field estimate for the critical temperature is therefore

$$T_c = z\,J = 2D\,J \tag{3.29}$$

From the Ising's exact solution for 1 dimension, the above expression is clearly incorrect as $T_c = 0$ in 1 dimension. In 2 dimensions, exact value is $T_c = 2.269\,J$ which is significantly lower than the mean field prediction of $4\,J$. In general, this indicates that in lower dimensions, fluctuations are

more important and tend to reduce the critical temperature by increasing disorder.

3.3.2 Critical Exponents in Mean Field Theory

For temperatures close to T_c and small $\beta|h|$ the value m_0 of the magnetization at the minimum of Landau function is small. We may therefore approximate the Landau function by expanding the right-hand side of Eq. (3.26) up to fourth order in m and linear order in h. We make use of the expansion

$$\ln[2\cosh(x)] = \ln 2 + \frac{x^2}{2} - \frac{x^4}{12} + \mathcal{O}(x^6) \tag{3.30}$$

to get

$$\mathscr{L}_{\mathrm{MF}}(T,h;m) = f + \frac{r}{2}m^2 + \frac{u}{4!}m^4 - hm + \ldots \tag{3.31}$$

Comparing the two expansions Eq. (3.30) and Eq. (3.31) above and using Eq. (3.26),

$$\begin{aligned} f &= -T\ln 2 && (3.32)\\ r &= \frac{zJ}{T}\left(T - zJ\right) \\ &\approx T - T_c && (3.33)\\ u &= 2T\left(\frac{zJ}{T}\right)^4 \\ &\approx 2T_c && (3.34) \end{aligned}$$

where the approximations are valid close to the critical temperature $T = T_c$ where $zJ/T \approx 1$. Then Eq. (3.27) simplifies to

$$r\,m_0 + \frac{u}{6}{m_0}^3 - h = 0 \tag{3.35}$$

The behavior of thermodynamic parameters close to T_c can be easily obtained. The values of critical exponents obtained from Mean Field Theory are $\alpha = 0$, $\beta = 1/2$, $\gamma = 1$ and $\delta = 3$ (the reader is referred to [Kop10] for a detailed derivation). Table bearing the exact experimental values for the exponents in dimensions two and three is shown below. A comparison with the mean field values shows that the Mean Field Approximation is not suitable to obtain quantitatively accurate results because of neglecting fluctuations especially in the physically accessible dimensions $D = 2$ and $D = 3$.

3.4 The Renormalization Group

The failure of Mean Field Theory in accurately predicting the critical exponents in dimensions $D < D_{up} = 4$ (the upper critical dimension) results from the fact that MFT can be shown to be

Table 3.1 Experimentally measured values of the critical exponents for the Ising model in dimensions 2 and 3. Source : [Kop10]

Exponent	$D=2$	$D=3$
α	0	0.110
β	1/8	0.3265
γ	7/4	1.2372
δ	15	4.789
ν	1	0.6301
η	1/4	0.0364

equivalent to the assumption that each spin on the lattice interacts equally with every other spin in the lattice implying infinite interaction range as $N \to \infty$, which is not physically possible. A more general approach to evaluating the macroscopic parameters of interacting many body systems is given by *the renormalization group* (or RG in short). In refers to a mathematical apparatus that allows systematic investigation of the changes of a physical system as viewed at different distance scales. The renormalization group has its origins in quantum field theory, but nowadays its applications extend to theory of condensed matter, solid-state physics, fluid mechanics, cosmology, high energy physics and even nanotechnology.

For a microscopic derivation of the critical behavior of thermodynamic observables, we have to calculate the partition function Z of the system. For Ising models, this amounts to performing the nested spin summations as described in the previous section. More generally, one can consider many-body systems whose partition function can be expressed in terms of some suitably defined functional path integral over a field Φ representing the relevant degrees of freedom,

$$Z(g) = \int \mathscr{D}[\Phi] e^{-S[\Phi;g]} \tag{3.36}$$

where $S[\Phi;g]$ is an effective action depending on a set of coupling constants collectively represented as the vector $g = (g_1, g_2, g_3, \dots)$. In case of the Ising model, the field Φ can be identified with the fluctutating order-parameter. However Eq. (3.36) is more general in the sense that the partition function of quantum many-body systems consisting of bosons, fermions and mixtures thereof can be written in this form (the path integral). Further to ensure relativistic covariance the fields Φ are considered to be functions of both position r and time t. Unfortunately in almost all cases of interest, the integration in Eq. (3.36) cannot be performed exactly, so one has to rely on approximations. Simple approximations such as the Mean Field Theory discussed above are very unreliable in systems

with dimensions less than D_{up}. The renormalization group then comes to the rescue.

3.4.1 The general RG procedure

The basic idea underlying the RG is conceptually very simple, although in practice it is usually rather difficult to carry out the RG procedure in practice.The strategy is to perform the integration over the degrees of freedom represented by the field Φ in Eq. (3.36) iteratively in small steps by integrating over suitably chosen subsets of fields and calculating the resulting change of the effective action. One iteration of the RG procedure consists of two major steps

3.4.1.1 Step 1 : Mode Elimination (Decimation)

The first RG step consists of the elimination of the degrees of freedom (also called modes) representing short-distance fluctuations involving a certain interval of small wavelengths. Sometimes, this is also called the *decimation* step. If we represent the partition function via a functional integral of the type (3.36) and work in momentum space, this means that we integrate over all fields $\Phi(k)$ with wave vectors k belonging to a certain high-momentum regime. There is considerable freedom in the choice of the high-momentum regime, and the most convenient choice depends on the model of interest and on the requirements on the accuracy of the calculation at hand. It is often convenient to integrate over fields $\Phi(k)$ whose wave vectors lie in the momentum shell $\Lambda < |k| < \Lambda_0$ where Λ is an ultraviolet cutoff. Formally, the separation into a small wave vector and a large wave vector regime amounts to writing the field Φ as a sum of two terms,

$$\Phi = \Phi^{<} + \Phi^{>} \tag{3.37}$$

where the smaller part $\Phi^{<}$ (slow modes) contains fluctuations with wave vectors smaller than a certain cutoff Λ, while the larger part $\Phi^{>}$ (fast modes) contains the complementary fluctuations involving large wave vectors. A simple way to implement the above decomposition is by multiplying the Fourier components $\Phi(k)$ in momentum space by $I = \Theta(\Lambda - |k|) + \Theta(|k| - \Lambda)$ so that

$$\begin{aligned} \Phi^{<}(k) &= \Theta(\Lambda - |k|)\Phi(k) \\ \Phi^{>}(k) &= \Theta(|k| - \Lambda)\Phi(k) \end{aligned} \tag{3.38}$$

where Θ stands for the Heaviside function. However such a sharp cutoff in momentum space sometimes lead to computational complications, which can be circumvented by smoothing out the boundary between integrated and unintegrated momenta. For low dimensional systems, it is advantageous to carry out the mode elimination step in real space which we will see in detail in the

next chapter. Formally, the mode-elimination step corresponds to the integration over the larger field component $\Phi^>$ in the functional integral,

$$\begin{aligned} Z &= \int \mathscr{D}[\Phi^<] \int \mathscr{D}[\Phi^>] e^{-S[\Phi^< + \Phi^>; g]} \\ &= \int \mathscr{D}[\Phi^<] e^{-S_\Lambda^<[\Phi^<; g^<]}, \end{aligned} \tag{3.39}$$

where we have defined

$$e^{-S_\Lambda^<[\Phi^<; g^<]} = \int \mathscr{D}[\Phi^>] e^{-S[\Phi^< + \Phi^>; g]}, \tag{3.40}$$

The coupling constants $g^<$ in $S^<[\Phi^<; g^<]$ will in general be different from the original couplings g, except in the case where $S[\Phi]$ is Gaussian so that the modes with different wave vectors (or frequencies) are not coupled. In practice the functional integration in Eq. (3.39) cannot be carried out exactly, so that approximations are necessary.

3.4.1.2 Step 2 : Rescaling

In the iterative second step of the RG procedure, we rescale wave vectors and fields and express the functional $S^<[\Phi^<; g^<]$ in terms of rescaled quantities such that it has the same functional form as Eq. (3.36) before the mode elimination. The combined effect of mode elimination and rescaling should then be taken into account via a modification of the coupling constants. Therefore, we define rescaled wave vectors k' via

$$k' = b\,k \tag{3.41}$$

where the dimensionless parameter $b = \Lambda_0/\Lambda$ defines the step size of the RG transformation. In wave vector space, the rescaled field $\Phi'(k')$ is related to the original field $\Phi^<(k')$ via

$$\Phi'(k') = \zeta_b^{-1} \Phi^<(k'/b) \tag{3.42}$$

where the rescaling factor ζ_b is in general a product of two factors,

$$\zeta_b = b^{D_\Phi} \sqrt{Z_b} \tag{3.43}$$

The first factor b^{D_Φ} is determined by the *normal dimension* D_Φ of the field $\Phi(k)$ which measures how many powers of inverse length are needed to make $\Phi(k)$ dimensionless. The value of D_Φ follows from the bare action by simple dimensional analysis. The second factor $\sqrt{Z_b}$ cannot be deduced by dimensional analysis and is closely related to the correlation function exponent η and the so-called

wave function renormalization factor Z_Φ in quantum mechanical many-body systems where it is called the *anomalous scaling dimension*.

3.4.1.3 Mathematical Formulation

The combination of the mode-elimination step with the rescaling step defines now a mapping between the initial couplings $g = (g_1, g_2, g_3, \dots)$ of a given model system with action $S[\Phi; g]$ and a modified set of couplings g' appearing in the new effective action $S'[\Phi'; g']$. The mapping can be expressed in vector form as

$$g' = \mathscr{R}(b; g) \tag{3.44}$$

The function $\mathscr{R}(b; g)$ represents an RG transformation acting on the space of coupling constants that specifies a specific model system. In general $\mathscr{R}(b; g)$ is a very complicated nonlinear function of the couplings g, whose precise form depends also on the length rescaling factor b. Mathematically, the set of transformations $\mathscr{R}(b; g)$ labeled by the continuous parameter b is a semigroup. Formally, the elimination of the short-wavelength fluctuations generates a projection of the coupling space defining the microscopic model onto a reduced coupling space associated with a new effective model with the same long-wavelength properties. The complete RG procedure is now defined by iterating the above two-step procedure, defining for given initial couplings $g^{(0)} = g$ a chain of renormalized couplings $g^{(n)}$ via

$$g^{(n)} = \mathscr{R}(b; g^{(n-1)}) = \mathscr{R}(b^n; g) \tag{3.45}$$

For $n \to \infty$ the total rescaling factor b^n diverges, which means that we have integrated out all degrees of freedom, so that in principle we can identify the field independent part $f^{(n)}$ of the resulting effective action for $n \to \infty$ with the exact free energy density of the system. However, in almost all physically interesting cases the RG transformation can only be carried out approximately, so that we cannot calculate the exact free energy in this way. The crucial point is, however, that the iteration of rather simple approximate RG transformations $\mathscr{R}(b; g)$ with a constant RG step size $b > 1$ can generate nonperturbative expressions for various physical quantities.

In practice, there are many different ways of implementing the RG procedure, for example, the mode-elimination step can be performed in real space, in wave vector space, or (for quantum systems) in frequency space. Moreover, there is some freedom in the choice of the RG step size b and there are many possibilities of introducing a cutoff Λ separating long-wavelength from short-wavelength fluctuations into a given model. Unfortunately, there is no unique implementation of the RG procedure which can be used as a black box in all situations. Instead, special versions of the RG procedure have proven to be useful to study certain classes of problems. The following diagram

shows a broad classification of the RG procedures used in practice. In order to develop the work

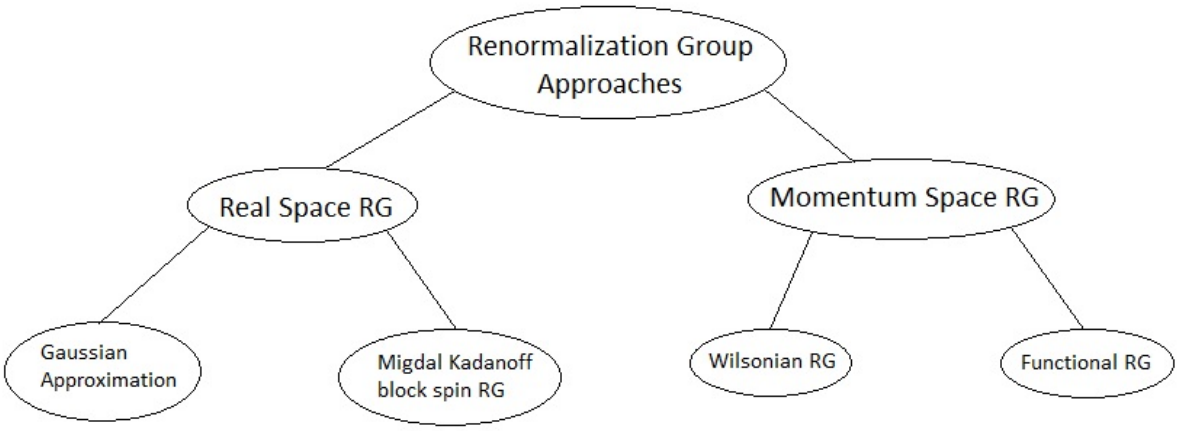

Figure 3.2 Classification of Renormalization Group Approaches. Source : [Kop10]

further, it is essential to understand the fundamentals and origins of the Renormalization Group. The next chapter introduces the tombstone of modern theoretical physics - the Quantum Field Theory and the origins of RG.

CHAPTER

4

RENORMALIZATION IN QFT

4.1 Perturbation Theory

Perturbation theory comprises mathematical methods for finding an approximate solution to a problem, by starting from the exact solution of a related problem. A critical feature of the technique is a step that breaks the problem into solvable and perturbation parts. Perturbation theory is applicable if the problem at hand cannot be solved exactly, but can be formulated by adding a small term to the mathematical description of the exactly solvable problem. Before going into the details of perturbation theory, it would be beneficial to introduce a labour saving device in mathematical physics invented in early nineteenth century by a Nottingham miller George Green called *Green's functions*.

4.1.1 Green's Functions

A Green's function is the impulse response of an inhomogenous differential equation defined on a domain, with specified initial conditions. Via the superposition principle, the convolution of a Green's function $G(x)$ with an arbitrary function $f(x)$ on that domain is the solution to the

inhomogenous differential equation for $f(x)$. Formally, for a partial differential equation of the form

$$L_x \Phi(x) = f(x) \tag{4.1}$$

where L_x is a differential operator which can be expressed as

$$L_x \equiv \sum_{k=0}^{n} a_k \left(\frac{\partial}{\partial x} \right)^k \tag{4.2}$$

One defines the Green's function as the solution of the following differential equation

$$L_x G(x - x') = \delta(x - x') \tag{4.3}$$

The solution of Eq. (4.1) is then given by

$$\Phi(x) = \int f(x') G(x - x') \mathrm{d}x' \tag{4.4}$$

Proof

Taking the fourier transform of Eq. (4.1) and using Eq. (4.2),

$$\left(a_0 \delta(\omega) + \sum_{k=1}^{n} a_k (i\omega)^k \right) \cdot \tilde{\Phi}(\omega) = \tilde{F}(\omega) \tag{4.5}$$

Hence,

$$\tilde{\Phi}(\omega) = \tilde{F}(\omega) \cdot \frac{1}{a_0 \delta(\omega) + \sum_{k=1}^{n} a_k (i\omega)^k} \tag{4.6}$$

From the fourier transform of Eq. (4.3),

$$\tilde{G}(\omega) = \frac{1}{a_0 \delta(\omega) + \sum_{k=1}^{n} a_k (i\omega)^k} \tag{4.7}$$

Using Eq. (4.7) in Eq. (4.6) and using the inverse fourier transform,

$$\Phi(x) = \int f(x') G(x - x') \mathrm{d}x'$$

Q.E.D

4.1.2 Perturbation Series (λ Expansion)

Assume that the differential operator L_x in Eq. (4.1) can be expanded as

$$L_x \equiv L_0 + \lambda L_I \tag{4.8}$$

where $\lambda \ll 1$ and the subscript I stands for interaction. The operator L_0 is such that one can easily solve the equation

$$L_0 \Phi_0(x) = f(x). \tag{4.9}$$

One can obtain the Green's function $G_0(x-x')$ corresponding to Eq. (4.9) such that

$$\Phi_0(x) = \int f(x') G_0(x-x') \mathrm{d}x' \tag{4.10}$$

We assume that the perturbed, or the exact solution $\Phi(x)$ has the form

$$\Phi(x) = \Phi_0(x) + \lambda \Phi_1(x) + \lambda^2 \Phi_2(x) + \ldots \tag{4.11}$$

to all orders in expansion parameter λ. As λ is small and if $\Phi_i(x)$ does not grow too fast, one can truncate the expansion at a low order. Using Eq. (4.11) in Eq. (4.1), we get

$$L_0\Phi_0(x) + \lambda L_0\Phi_1(x) + \lambda^2 L_0\Phi_2(x) + \lambda L_I\Phi_0(x) + \lambda^2 L_I\Phi_1(x) + \mathcal{O}(\lambda^3) = f(x) \tag{4.12}$$

By equating the powers of λ on both sides of Eq. (4.12) and using Eq. (4.11),

$$\Phi(x) = G_0(x)\big[1 - \lambda L_I G_0(x) + \lambda^2 L_I G_0(x) L_I G_0(x) + \mathcal{O}(\lambda^3)\big] f(x). \tag{4.13}$$

4.1.3 Limitations of Perturbation Theory

There are three problems that afflict the use of perturbation theory in practice

1. Coefficients in the λ expansion may depend on integrals which are divergent.
2. If λ is not very small, one cannot truncate the perturbation expansion at low order.
3. When one goes beyond the purely symbolic treatment presented in Eq. (4.11) to Eq. (4.13), terms at each order of λ can be very intricate mathematically and the complexity increases rapidly with the power of λ.

Methods have been found for tackling all of these problems, mostly which are ad-hoc in nature and can be collectively lumped together under the title of *renormalized perturbation theory* which, as

we will see, is the precursor of the Wilson's renormalization group.

4.2 Quantum Field Theory

4.2.1 Klein-Gordon Equation

The Klein-Gordon Lagrange density for a relativistic scalar field is given by

$$\mathscr{L} = \frac{1}{2}\partial^{\mu}\Phi \cdot \partial_{\mu}\Phi - \frac{1}{2}m^2\Phi^2 - V(\Phi), \tag{4.14}$$

where V is the potential as a function of the field $\Phi(x)$ defined over all points x in the d dimensional space-time. From the Hamilton's principle of stationary action, the Euler Lagrange equations of motion for the Lagrange density Eq. (4.14) yield

$$\left[\partial_{\mu}\partial^{\mu} + m^2\right]\Phi = -\frac{\partial V}{\partial \Phi}. \tag{4.15}$$

One is specially interested in the case of free field (i.e. $V = 0$) which is described by the free field Klein-Gordon equation

$$\left[\partial_{\mu}\partial^{\mu} + m^2\right]\Phi = 0. \tag{4.16}$$

4.2.1.1 Feynman Propagator

Using the theory of Green's functions outlined above and working in the fourier transformed wave vector space for the Klein-Gordon equation Eq. (4.16),

$$\left[-k^2 + m^2\right]\Delta_F = -1 \tag{4.17}$$

where Δ_F is the causal Green's function and the negative sign on the right side is just a matter of convention. Working in the units where $\hbar = c = 1$, and making sure that causality is not violated, the inverse Fourier transform of Δ_F takes the form of a contour integral

$$\Delta_F(x-y) = \lim_{\epsilon \to 0} \frac{1}{(2\pi)^4} \oint \mathrm{d}^4k \frac{e^{-ik(x-y)}}{k^2 - m^2 + i\epsilon} \tag{4.18}$$

Causality is ensured by picking up the right poles during the upper and lower halves of the contour integral. The infinitesimal term $i\epsilon$ enables one to evaluate the causal Green's function, henceforth called the *Feynman Propagator*. If J (called the source field) is an element of the dual space of the

field configurations Φ, then, the generating functional Z of the source fields is defined by

$$Z[J] = \int \mathscr{D}\Phi e^{iS[\Phi]+\langle J,\Phi\rangle}, \tag{4.19}$$

where the functional integral Eq. (4.19) is carried out over all possible field configurations, $S[\Phi]$ is the action corresponding to the Klein Gordon Lagrange density and $\langle *,*\rangle$ represents inner product over the entire space-time. For the free field case, using the canonical quantization relations, one can show that

$$\begin{aligned} G_0(x-y) &= \left\langle 0\middle|\mathscr{T}\{\Phi(x)\Phi(y)\}\middle|0\right\rangle & (4.20)\\ &= i\Delta_F(x-y), & (4.21)\end{aligned}$$

where $G_0(x-y)$ is the vacuum expectation value of the time ordered product of the field operator Φ at space-time coordinates x and y. This quantity represents a 2-point correlation function of the field operator and is also called the *bare propagator*.

4.2.1.2 Wick Rotation and Connected Green's Function

Before we proceed further, it is interesting to discuss another powerful mathematical tool known as *Wick rotation*. Wick rotation is a method of finding solution to a problem in the Minkowski space by solving a related problem in the Euclidean space by applying a transformation that substitutes an imaginary-number variable for a real-number variable. Wick rotation is motivated by the observation that the Minkowski metric (with $(-1,+1,+1,+1)$ convention for the metric tensor) given by

$$\mathrm{d}s^2 = -\mathrm{d}t^2 + \sum\nolimits_i \mathrm{d}x_i{}^2 \tag{4.22}$$

and the four-dimensional Euclidean metric given by

$$\mathrm{d}s^2 = \mathrm{d}\tau^2 + \sum\nolimits_i \mathrm{d}x_i{}^2 \tag{4.23}$$

are equivalent if one permits the time coordinate t to take on imaginary values. The Minkowski metric becomes Euclidean when t is restricted to the imaginary axis, and vice versa. Taking a problem expressed in Minkowski space with coordinates (x_i, t), and substituting $t = -i\tau$, sometimes yields a problem in real Euclidean coordinates (x_i, τ) which is easier to solve. This solution may then, under reverse substitution, yield a solution to the original problem. Henceforth we will only work in the

Wick rotated Euclidean space. In this space,

$$G_0(x-y)=\Delta_F(x-y). \tag{4.24}$$

Hence the bare propagator is the same as the Feynman propagator in the wick rotated space and the generating functional Eq. (4.19) takes the following form

$$Z[J]=\int \mathscr{D}\Phi e^{-H[\Phi]+\langle J,\Phi\rangle}, \tag{4.25}$$

where the action $S[\Phi]$ is replaced by the Hamiltonian $H[\Phi]$ and the imaginary factor i has been replaced by -1. The Green's function for the interacting fields can be obtained from Eq. (4.25) as

$$G(x-y)=\left(\frac{\delta}{\delta J(x)}\right)\left(\frac{\delta}{\delta J(y)}\right)Z[J]\bigg|_{J=0}, \tag{4.26}$$

One of the problems with using the above formulation Eq. (4.26) is that it is not normalized. One can define a normalized quantity called the *exact n-point correlation* or the n-point connected Green's function as

$$G^{(n)}(x_1,x_2,\ldots,x_n)=\frac{1}{Z[J]}\left(\frac{\delta}{\delta J(x_1)}\right)\left(\frac{\delta}{\delta J(x_2)}\right)\ldots\left(\frac{\delta}{\delta J(x_n)}\right)Z[J]\bigg|_{J=0}. \tag{4.27}$$

4.2.2 Φ^4 Scalar Field Theory

A very well studied quantum field theory is the Φ^4 scalar field theory. It is called so because of the potential term in its Lagrange density functional which is given in the Minkowski space as

$$\mathscr{L}=\frac{1}{2}\partial^\mu\Phi\cdot\partial_\mu\Phi-\frac{1}{2}m^2\Phi^2-\frac{\lambda_0}{4!}\Phi^4. \tag{4.28}$$

Using Eq. (4.25), the generating functional $Z[J]$ for the Φ^4 theory in wick rotated Euclidean space is given by

$$Z[J]=\int \mathscr{D}\Phi e^{-H_0[J]}\exp\Big[-\int \mathrm{d}^D x\ \frac{\lambda_0}{4!}\Phi^4\Big]. \tag{4.29}$$

Expand the second exponential in Eq. (4.29) in powers of λ_0 giving

$$Z[J]=\int \mathscr{D}\Phi e^{-H_0[J]}\Big[\sum_{n=0}^{\infty}\frac{1}{n!}\Big(-\frac{\lambda_0}{4!}\int \mathrm{d}^D x\ \Phi^4\Big)^n\Big] \tag{4.30}$$

Exchanging the order of summation and integration in Eq. (4.30) and multiplying r.h.s above and below by the free field generating functional $Z_0[J]$ yields

$$Z[J] = Z_0[J]\sum_{n=0}^{\infty}\frac{1}{n!}\left\langle\left(-\frac{\lambda_0}{4!}\int \mathrm{d}^D x\ \Phi^4\right)^n\right\rangle_0, \tag{4.31}$$

where $\langle\ldots\rangle_0$ denotes the Gaussian average or the vacuum expectation value (VeV). From the derivation in [Ste93], we also have

$$\begin{aligned} Z_0[J] &= Z_0[0]\exp\left[\frac{1}{2}\iint \mathrm{d}^D x\,\mathrm{d}^D y\ J(x)\Delta(x-y)J(y)\right] &(4.32)\\ &= Z_0[0]\exp\left[\frac{1}{2}J\Delta J\right], &(4.33)\end{aligned}$$

where the form on the second line is the DeWitt notation. Thus from Eq. (4.31) and Eq. (4.32),

$$Z[J] = Z_0[J]\exp\left[-\frac{\lambda_0}{4!}\int \mathrm{d}^D x\ \frac{\delta^4}{\delta J^4(x)}\right]\exp\left[\frac{1}{2}\iint \mathrm{d}^D x\,\mathrm{d}^D y\ J(x)\Delta(x-y)J(y)\right] \tag{4.34}$$

By expanding out the exponentials in Eq. (4.34), we can obtain a power series in λ_0 for $Z[J]$. Now consider the exact 2-point correlation function (also called the exact propagator) given by

$$G^{(2)}(x_1,x_2) = \frac{1}{Z[J]}\left(\frac{\delta}{\delta J(x_1)}\right)\left(\frac{\delta}{\delta J(x_2)}\right)Z[J]\Big|_{J=0} \tag{4.35}$$

Expanding $Z[J]$ in Eq. (4.35) as a power series in λ_0 up to $\mathcal{O}({\lambda_0}^2)$, we obtain the following after some algebra

$$G^{(2)}(x_1,x_2) = \Delta(x_1-x_2) + \frac{\lambda_0}{2}\int \mathrm{d}^D x\ \Delta(x_1-x)\Delta(x-x)\Delta(x-x_2) + \mathcal{O}({\lambda_0}^2) \tag{4.36}$$

The terms that do not propagate from x_1 to x_2 in the expansion of the original unnormalized propagator in terms of the bare propagator are called *vacuum fluctuations*. The normalization by $Z[J]$ removes these non-propagating terms in the exact 2-point correlation function.

4.2.3 Feynman Diagrams for Loop Corrections

The terms to any order in the expansion Eq. (4.36) can be worked out by a simple set of rules, with the numerical coefficients being determined by purely combinatoric operations. For this reason, it is only the topology of a term that matters and this fact can be exploited if the algebraic terms are replaced by ,what are better known collectively as, *Feynman Diagrams*. For the perturbative (loop)

corrections to the bare propagator, they can be constructed by the following set of rules

1. Represent a coordinate by a dot.
2. Represent a bare propagator $\Delta(x_1 - x_2)$ by a line segment joining two dots.
3. Any dot which is common to two or more segments is a variable which is integrated over.
4. A bare propagator term between a coordinate and itself (i.e. of the form $\Delta(x-x)$) is represented by a loop.
5. Number of segments (loops) between (at) two (one) coordinate(s) is given by the power to which the corresponding bare propagator is raised in the expansion of the 2-point correlation Eq. (4.36)

Using these, one can write the perturbation expansion for any exact propagator (or connected Green's function) to any order. The expansion of $G^{(2)}(x_1, x_2)$ up to $\mathcal{O}({\lambda_0}^3)$ Eq. (4.36) can be expressed as the following using Feynman Diagrams The diagrams remain the same in both real and wave

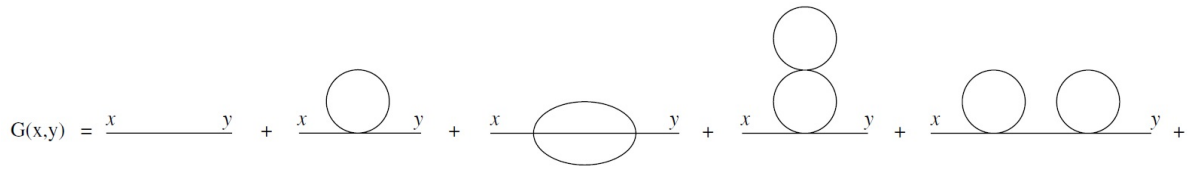

Figure 4.1 Diagrams representing the exact 2-point correlation function up to $\mathcal{O}({\lambda_0}^3)$. Source : [McC04]

vector space, with small changes in the labeling. The first order expression for $G^{(2)}(x_1, x_2)$ can be written in wave number space as

$$G^{(2)}(k) = G_0(k) + \frac{\lambda_0}{2} G_0(k) \left[\int \mathrm{d}^D q \; G_0(q) \right] G_0(k) + \mathcal{O}({\lambda_0}^2) \tag{4.37}$$

The rules for writing down the expansion in wave vector space from the Feynman diagrams are

1. A vertex represents a factor of λ_0
2. A line represents a factor of $G_0(k)$
3. A loop represents an integral $\int \mathrm{d}^D q$

4. Every graph is multiplied by a symmetry factor which is evaluated using *Wick's Theorem* for Gaussian correlations [Kop10].

One can further note that in the expansion of the original Green's function, in addition to vacuum fluctuations, some diagrams are disconnected; i.e., made up of a number of sub-diagrams which are not connected together. The terms in the (real space) expansion that have multiplications form disconnected diagrams, while the terms that have only convolutions are called connected diagrams. Henceforth, we will only concentrate on connected diagrams, as the expansions of the connected Green's functions only have these. These connected diagrams can be further categorized into

1. One-particle reducible (1 - PR) diagrams: These are the ones wherein cutting a single internal line produces two disconnected diagrams.

2. One-particle irreducible (1 - PI) diagrams: The diagrams which are not 1 - PR.

1 - PI diagrams lead to very important building blocks of the connected Green's function called *proper vertex functions*. They are the sum of all 1 - PI diagrams in expansion of the connected Green's function with external lines cut off (amputated). The only exception to this rule is the 2-vertex given by

$$\Upsilon^{(2)}(k) = {G_0}^{-1}(k) - \Sigma(k) \tag{4.38}$$

The term $\Sigma(k)$ in Eq. (4.38) is called the irreducible self-energy. It is the sum of all amputated diagrams in the expansion of $G^{(2)}(k)$. The latter can be expressed as

$$G^{(2)}(k) = G_0(k) + G_0(k)\Sigma(k)G^{(2)}(k) \tag{4.39}$$

From Eq. (4.38) and Eq. (4.39), we get

$$\Upsilon^{(2)}(k) = \frac{1}{G^{(2)}(k)} \tag{4.40}$$

Just as $\ln\big(Z[J]\big)$ serves as the generating functional for the n-point correlation function, the generating functional for the n-point proper vertex is the *Effective Action* functional $\Upsilon[\bar{\Phi}]$, given by the Legendre transform of $\ln\big(Z[J]\big)$

$$\Upsilon[\bar{\Phi}] = \int \mathrm{d}^D x \; J(x)\bar{\Phi}(x) - \ln\big(Z[J]\big) \tag{4.41}$$

where $\bar{\Phi}$ is the VeV of the field operator

$$\bar{\Phi}(x) = \frac{\delta \ln\big(Z[J]\big)}{\delta J(x)} \tag{4.42}$$

The n-point proper vertex functions are then obtained from the effective action $\Upsilon[\bar{\Phi}]$ as

$$\Upsilon^{(n)}(k_1, k_2, \ldots, k_n) = \left(\frac{\delta}{\delta\bar{\Phi}(-k_1)}\right)\left(\frac{\delta}{\delta\bar{\Phi}(-k_2)}\right)\ldots\left(\frac{\delta}{\delta\bar{\Phi}(-k_n)}\right)\Upsilon[\bar{\Phi}]\Big|_{\bar{\Phi}=0} \tag{4.43}$$

4.3 Renormalization in Φ^4 Field Theory

This section follows the development in [Kop10]

4.3.1 Perturbative Renormalization

The momentum integrals in the expansion of the connected Green's functions are unrestricted, which leads to *ultraviolet divergences* in Field Theory. To the first order in λ_0, the evaluation of self energy $\Sigma(k)$ is given by

$$\begin{aligned}
\Sigma(k) &= \frac{\lambda_0}{2}\int \mathrm{d}^D k\ \frac{1}{k^2 + m_0^2} \\
&= \frac{\lambda_0}{2} K_d\, m_0^{D-2} \int_0^\infty \mathrm{d}q\ \frac{q^{D-1}}{1+q^2} \\
&= \infty, \quad \forall\, D \geq 2
\end{aligned} \tag{4.44}$$

where

$$K_d = \frac{1}{(2\pi)^{(D/2)}\Gamma\left(\frac{D}{2}\right)} \tag{4.45}$$

where Γ is the *Reimann Gamma* function

$$\Gamma(t) = \int_0^\infty \mathrm{d}x\ x^{t-1} e^{-x} \tag{4.46}$$

We can have a similar analysis for the proper 4-vertex. To $\mathcal{O}({\lambda_0}^2)$,

$$\begin{aligned}\Upsilon^{(4)}(k_1,k_2,k_3,k_4) &= -\frac{3{\lambda_0}^2}{2}\int \mathrm{d}^D k\,\frac{1}{[k_2+m_0^2]^2}\\ &= -\frac{3{\lambda_0}^2}{2}K_d\, m_0^{D-4}\int_0^\infty \mathrm{d}q\,\frac{q^{D-1}}{[1+q^2]^2}\\ &= \infty, \quad \forall\, D\geq 4 \end{aligned} \tag{4.47}$$

In order to manipulate these divergent integrals appearing in the perturbation expansion, we have to make them finite as intermediate stages of calculation by introducing some ultraviolet cutoff on the momentum integral. This is called *regularization*. At the end of the calculation, we should be able to somehow remove these artificial cutoffs to obtain a renormalized theory which is independent of this cutoff scale. One can use a sharp momentum cutoff Λ. However, for calculations beyond one loop order the non-analyticity of the sharp cutoff gives rise to complications, so in practice, it is better to work with a smooth cutoff such as a Gaussian momentum cutoff

$$\int \frac{\mathrm{d}^D k}{(2\pi)^d} \to \int \frac{\mathrm{d}^D k}{(2\pi)^d} e^{-k^2/\Lambda^2} \tag{4.48}$$

Using Eq. (4.48) in Eq. (4.44) and Eq. (4.47) for $d=4$, we get the following for the self energy $\Sigma(k)$ and the 4-vertex $\Upsilon^{(4)}$ up to a leading order in λ_0

$$\Sigma(k) = \frac{K_4}{2}\lambda_0\left[\frac{\Lambda^2}{2}-m_0^2\ln\left(\frac{\Lambda}{m_0}\right)+\mathcal{O}(1)\right] \tag{4.49}$$

$$\Upsilon^{(4)}(k_1,k_2,k_3,k_4) \approx -\frac{3K_4}{2}{\lambda_0}^2\ln\left(\frac{\Lambda}{m_0}\right)+\mathcal{O}(1) \tag{4.50}$$

In order to remove the terms dependent on cut-off from Eq. (4.49) and Eq. (4.50), one introduces the so-called renormalized Lagrangian expressed as a function of the renormalized field Φ_R, the renormalized mass m_R, and the renormalized coupling λ_R. These renormalized quantities are related to the bare quantities as

$$\Phi_0 = \sqrt{Z_\Phi}\Phi_R \tag{4.51}$$

$$m_0^2 = Z_m m_R^2 \tag{4.52}$$

$$\lambda_0 = Z_\lambda \lambda_R \tag{4.53}$$

where the dimensionless multiplicative renormalization constants $\{Z\}$ will be determined iteratively order by order in perturbation theory. The general strategy then is to absorb all infinities into these constants. The idea is that only renormalized quantities have a physical meaning and can be related to physical observables. We can express the original Lagrange density Eq. (4.28) (Hamiltonian density in the wick rotated space) in terms of renormalized quantities as follows

$$H_0[\Phi] = \frac{1}{2}\Big[\big(\nabla\Phi_R\big)^2 + m_R^2{\Phi_R}^2\Big] + \frac{\lambda_R}{4!}{\Phi_R}^4 + \chi[\Phi] \tag{4.54}$$

where $\chi[\Phi]$ consists of the following counter terms

$$\chi[\Phi] = \frac{1}{2}\big(Z_\Phi - 1\big)\big(\nabla\Phi_R\big)^2 + \frac{1}{2}\big(Z_m Z_\Phi - 1\big)m_R^2\Phi^2 + \big(Z_\lambda {Z_\Phi}^2 - 1\big)\frac{\lambda_R}{4!}{\Phi_R}^4 \tag{4.55}$$

The first three terms on the right side of Eq. (4.54) are of the same form as the bare Hamiltonian density, but with bare quantities replaced with renormalized ones. The counter terms Eq. (4.55) are considered to be a part of the interaction in the perturbative renormalization. One can expand the Z factors in powers of renormalized coupling λ_R to obtain a series of the form

$$Z_i = 1 + \sum_{\nu=1}^{\infty} C_i^{(\nu)}(m_R, \mu, \Lambda)\,\lambda_R^\nu \quad i = \Phi, m, \lambda \tag{4.56}$$

The crucial step now is to choose the coefficients $C_i^{(\nu)}$ such that the perturbative expansion of the renormalized Hamiltonian density Eq. (4.54) is finite. Any singularity encountered is absorbed in the Z-factors. Using the expansions of self energy Eq. (4.49) and 4-vertex Eq. (4.50), and placing the constraint that the renormalized values of these two quantities are finite, we get

$$Z_m = 1 + \lambda_R\left[\frac{K_4}{2}\ln\left(\frac{\Lambda}{m_R}\right) - \frac{\Lambda^2}{2m_R} + c_m^{(1)}\right] \tag{4.57}$$

$$Z_\lambda = 1 + \left[\frac{3K_4}{2}\ln\left(\frac{\Lambda}{m_R}\right) + c_\lambda^{(1)}\right] \tag{4.58}$$

$$Z_\Phi = 1 + \mathcal{O}({\lambda_R}^2) \tag{4.59}$$

where $c_i^{(1)}$ denote the non-singular part of $C_i^{(1)}$, for all the Z-factors Z_i, which remains finite for $\Lambda \to \infty$ and is arbitrary otherwise. Eq. (4.59) arises from the fact that the self energy is momentum independent to $\mathcal{O}(\lambda_R)$. This iterative procedure of calculating the renormalization factors can in principle be carried out to arbitrary high orders in λ_R. The important point is that for doing the calculation to a given order we do not need to know in advance the counterterms to this order;

they are obtained while doing the calculation. As the non-singular parts of the coefficients $C_i^{(1)}$ are arbitrary, they can be set to zero and this renormalization scheme is called *minimum subtraction*. Other renormalization schemes are also possible.

4.3.2 Callan-Symanzik Equation

The *Callan-Symanzik equation* relates the correlation functions calculated using renormalized perturbation theory for different values of renormalization parameters m_R, λ_R. Taking into account the relation between bare Φ_0 and renormalized fields Φ_R, the relation between bare and renormalized n-point vertex functions [Kop10] is given by

$$\Upsilon_0{}^{(n)}(k_1, k_2, \ldots, k_n; m_0, \lambda_0) = Z_\Phi^{-n/2} \Upsilon_R{}^{(n)}(k_1, k_2, \ldots, k_n; m_R, \lambda_R, \mu) \tag{4.60}$$

where μ represents the energy (cutoff) scale. Now, we desire that the left hand side of Eq. (4.60) to be independent of the scale μ which gives the following

$$\left[\mu \frac{\partial}{\partial \mu} + \beta \frac{\partial}{\partial \lambda_R} + \gamma m_R^2 \frac{\partial}{\partial m_R^2} - \frac{n}{2}\eta\right] \Upsilon_R{}^{(n)}(k_1, k_2, \ldots, k_n; m_R, \lambda_R, \mu) = 0 \tag{4.61}$$

Eq. (4.61) is the Callan-Symanzik equation for the renormalized proper vertex functions. Here,

$$\eta = \left.\frac{\partial \ln Z_\Phi}{\partial \ln \mu}\right|_{m_0, \lambda_0} \tag{4.62}$$

is the anomalous scaling dimension of the field. The *Gell Mann-Low beta* function is given by

$$\beta = \left.\frac{\partial \ln \lambda_R}{\partial \ln \mu}\right|_{m_0, \lambda_0} \tag{4.63}$$

and the function

$$\gamma = \left.\frac{1}{m_R^2} \frac{\partial \ln m_R^2}{\partial \ln \mu}\right|_{m_0, \lambda_0} \tag{4.64}$$

is responsible for renormalization of mass. The zeroes of the Beta function Eq. (4.63) are the fixed points of the Renormalization Group transformations. If the fixed point reached is non-trivial, then at that fixed value of the coupling λ_R and consequently fixed m_R^2/μ^2 , the field theory enjoys a symmetry known as the scale symmetry. If the field theory is relativistic, and the total Energy is conserved, it enjoys symmetry under the *Poincare group*. If scaling transformations are combined with translations and Lorentz transformations of the Poincare group, the resulting group is incomplete and requires the *Special Conformal Transformations* for completion. The resulting complete

group is known as the *Conformal group*. Symmetry under the conformal group is an important property of physical systems at the critical point of a second order phase transition and the branch of Condensed matter physics that deals with these phenomena is known as Conformal Field Theory.

CHAPTER

5

RG AND LEARNING

A central goal of modern machine learning research is to learn and extract important features directly from data. Among the most promising and successful techniques for accomplishing this goal are those associated with the emerging sub-discipline of deep learning. Despite the enormous success of deep learning, relatively little is understood theoretically about why these techniques are so successful at feature learning and compression. In [MS14], the authors show that deep learning is intimately related to the renormalization group (RG). They use the real space RG method introduced by Kadanoff and Migdal to demonstrate an exact mapping between RG and Deep Learning architectures based on Restricted Boltzmann Machines (RBMs). The relations developed in this chapter show how Conformal Symmetry develops in connectionist architectures which maximize the Entropic Utility Eq. (2.39) furnished by CEF. This is accomplished using the Functional Renormalization Group (FRG) and the thermodynamic *Massieu Function*, which is a statistical generalization of entropy production for systems evolving towards nonequilibrium steady states (NESS). FRG flow equation is called the Wetterich Equation after the founder Chritoph Wetterich. This RG approach is extremely general in that it combines methods of quantum field theory with the intuitive RG ideas of Kenneth Wilson (Wilsonian RG) [Kop10]. This generality makes FRG particularly powerful and it therefore finds applications in fields ranging from statistical field theory to theory of condensed matter, non-abelian gauge theories (e.g., Yang Mills theory), supersymmetry and the

renormalizability of quantum gravity.

5.1 Kadanoff RG and Deep Learning

Deep learning (Deep Neural Networks) uses multiple layers of representation to learn descriptive features directly from training data. They are biologically-inspired graphical statistical models that consist of multiple layers of 'neurons', with units in one layer receiving inputs from units in the layer below them. They can be viewed as an iterative coarse-graining scheme, where each new high-level layer of the neural network learns increasingly abstract higher level features from the data. By successively applying feature extraction, DNNs learn to deemphasize irrelevant features in the data while simultaneously learning relevant ones. This successive coarse-graining procedure is reminiscent of the renormalization group. In [MS14], the authors describe the use of Kadanoff real space RG scheme for spin systems to formally establish the mapping.

5.1.1 Kadanoff real space RG for Ising model

Kadanoff's variational RG scheme introduces coarse-grained auxiliary, or "hidden", spins that are coupled to the physical spin systems through some unknown coupling parameters. A parameter-dependent free energy is calculated for the coarse-grained spin system from the coupled system by integrating out the physical spins. The coupling parameters are chosen through a variational procedure that minimizes the difference between the free energies of the physical and hidden spin systems, which ensures that the coarse-grained system preserves the long-distance information present in the physical system. Carrying out this procedure results in an RG transformation that maps the physical spin system into a coarse-grained description in terms of hidden spins. The hidden spins then serve as the input for the next round of renormalization. In order to develop the connect between RG and Deep Learning, consider the conventional Ising partition function

$$Z = \mathrm{Tr}_{v_i} e^{-\mathrm{H}(\{v_i\})} \equiv \sum_{v_1,\ldots v_N=\pm 1} e^{-\mathrm{H}(\{v_i\})} \tag{5.1}$$

where we have set the temperature $T = 1$ in the Gibbs distribution Eq. (5.1) without loss of generality. One can thus describe the Free energy using the bridge equation as

$$F^{v} = -\log Z = -\log\left(\mathrm{Tr}_{v_i} e^{-\mathrm{H}(\{v_i\})}\right). \tag{5.2}$$

We can introduce $M < N$ new binary spins, h_j. Each of these spins h_j will serve as a coarse-grained degree of freedom where fluctuations on small scales have been averaged out. This is the mode

elimination (or decimation step) for this scheme. Such decimation typically increases the characteristic length of the system (the lattice spacing in this case). The coarse-grained Hamiltonian takes the form:

$$\mathrm{H}^{RG}[\{h_j\}] = -\sum_i K'_i h_i - \sum_{ij} K'_{ij} h_i h_j - \sum_{ijk} K'_{ijk} h_i h_j h_k + \ldots \tag{5.3}$$

where $\{K'\}$ describe the interactions (modified couplings) between hidden spins. In Kadanoff's scheme, the coarse graining is implemented by constructing a function $\mathrm{T}_\lambda(\{v_i\},\{h_j\})$, which depends on a set of variational parameters $\{\lambda\}$ and encodes the interactions between a set of hidden spins $\{h_j\}$ and a set of physical spins $\{v_i\}$, one can then marginalize over (integrate out) the visible spins to arrive at a description that solely depends on the hidden spins. According to [MS14], T_λ defines a Hamiltonian for the hidden spins through the expression

$$e^{-\mathrm{H}^{RG}_\lambda[\{h_j\}]} = \mathrm{Tr}_{v_i}\, e^{\mathrm{T}_\lambda(\{v_i\},\{h_j\})-\mathrm{H}(\{v_i\})}. \tag{5.4}$$

The free energy for the coarse grained system is then given by the bridge equation

$$F^h_\lambda = -\log\left(\mathrm{Tr}_{h_i}\, e^{-\mathrm{H}^{RG}_\lambda(\{h_i\})}\right). \tag{5.5}$$

It has to be ensured that the long-distance (large scale) physical observables of the system remain unchanged under the coarse graining transformation. All macroscopic observables for a thermodynamic system at equilibrium can be obtained from the partition function and hence from the free energy. Thus the parameters $\{\lambda\}$ need to be chosen in such a manner that the free energy difference, $\Delta F = F^h_\lambda - F^v$ between the coarse grained and fine grained descriptions of the system is minimized. So for an *exact* transformation, from Eq. (5.5), the requirement is that

$$\mathrm{Tr}_{h_j}\, e^{\mathrm{T}_\lambda(\{v_i\},\{h_j\})} = 1. \tag{5.6}$$

5.1.2 Deep Neural Networks and Restricted Boltzmann Machines

Restricted Boltzmann Machines (RBMs) are generative stochastic artificial neural networks that can learn a probability distribution over its set of inputs. RBMs are a variant of Boltzmann machines with the restriction that their neurons have bidirectional connections between layers. The units in the input layer are called *visible* units and units in the hidden layer are called *hidden units*. There are no connections amongst the units in a layer and the connections between the units of the two layers may be symmetric. *Deep Belief Networks* can be thought of as stacked RBMs, which are trained using gradient-descent and back-propagation layer by layer. To further the analogy between Kadanoff RG and Deep Learning, [MS14] assumes use of RBMs acting on binary data drawn from some probability

distribution $P(\{v_i\})$ with visible units (binary spins) $\{v_i\}$. For binary input data such as a black and white image, each pixel is on or off and the distribution $P(\{v_i\})$ encodes the statistical properties of an ensemble (dataset) of images. The hidden units $\{h_j\}$ model the data distribution by coupling to (connecting with) the visible units. The hidden layer of one RBM serves as the visible layer for other in case of stacked RBMs. The interactions between the hidden and visible units are modeled using an energy function of the form

$$\mathrm{E}(\{v_i\},\{h_j\}) = \sum_j b_j h_j + \sum_{ij} v_i w_{ij} h_j + \sum_i c_i v_i \tag{5.7}$$

where $\lambda = \{b_j, w_{ij}, c_i\}$ are the variational parameters of the model. Under this model, the joint probability of observing a configuration of hidden and visible spins is given by

$$p_\lambda(\{v_i\},\{h_j\}) = \frac{e^{-\mathrm{E}(\{v_i\},\{h_j\})}}{Z}. \tag{5.8}$$

This joint probabiltiy also defines a marginal probability over only visible or hidden spins as

$$p_\lambda(\{v_i\}) = \mathrm{Tr}_{h_j} p_\lambda(\{v_i\},\{h_j\}) \tag{5.9}$$

$$p_\lambda(\{h_j\}) = \mathrm{Tr}_{v_i} p_\lambda(\{v_i\},\{h_j\}). \tag{5.10}$$

Based on these marginal probabilities, one can define variational RBM Hamiltonians over visible and hidden spins by

$$p_\lambda(\{v_i\}) \equiv \frac{e^{-\mathrm{H}_\lambda^{RBM}[\{v_i\}]}}{Z} \tag{5.11}$$

$$p_\lambda(\{h_j\}) \equiv \frac{e^{-\mathrm{H}_\lambda^{RBM}[\{h_j\}]}}{Z}. \tag{5.12}$$

The objective of the RBM is to minimize the Kullback-Leibler divergence between the true distribution of the data $P(\{v_i\})$ and the marginal distribution $p_\lambda(\{v_i\})$. The KL divergence is given by

$$\mathrm{D}_{KL}(P \parallel p_\lambda) = \sum_{v_i} P(\{v_i\}) \log\left(\frac{P(\{v_i\})}{p_\lambda(\{v_i\})}\right) \tag{5.13}$$

In general it is not possible to explicitly minimize the KL divergence Eq. (5.13) and it is usually performed using approximate numerical methods.

5.1.3 Mapping RG to Deep Learning

As presented in the sections above, there is a strong relation between the operators $\mathrm{T}_\lambda(\{v_i\},\{h_j\})$ in RG and the joint energy function $\mathrm{E}(\{v_i\},\{h_j\})$ in RBMs. Mathematically,

$$\mathrm{T}_\lambda(\{v_i\},\{h_j\}) = -\mathrm{E}(\{v_i\},\{h_j\}) + \mathrm{H}(\{v_i\}). \tag{5.14}$$

The above equation defines the mapping between the RG scheme and RBM based deep networks. Dividing Eq. (5.4) by Z (the partition function), one gets

$$\frac{e^{-\mathrm{H}_\lambda^{RG}[\{h_j\}]}}{Z} = \frac{\mathrm{Tr}_{v_i} e^{\mathrm{T}_\lambda(\{v_i\},\{h_j\})-\mathrm{H}(\{v_i\})}}{Z} \tag{5.15}$$

Substituting Eq. (5.14) in Eq. (5.15) yields

$$\begin{aligned} \frac{e^{-\mathrm{H}_\lambda^{RG}[\{h_j\}]}}{Z} &= \frac{\mathrm{Tr}_{v_i} e^{-\mathrm{E}(\{v_i\},\{h_j\})}}{Z} \\ &= p_\lambda(\{h_j\}) \end{aligned} \tag{5.16}$$

Eq. (5.16) and Eq. (5.12) then yield

$$\mathrm{H}_\lambda^{RG}[\{h_j\}] = \mathrm{H}_\lambda^{RBM}[\{h_j\}] \tag{5.17}$$

which means that the RG Hamiltonian is the same as the variational Hamiltonian in RBMs. Using Eqs. (5.8), (5.9) and (5.14), one further notices that

$$\begin{aligned} e^{\mathrm{T}_\lambda(\{v_i\},\{h_j\})} &= e^{-\mathrm{E}(\{v_i\},\{h_j\})+\mathrm{H}[\{v_i\}]} \\ &= \frac{p_\lambda(\{v_i\},\{h_j\})}{p_\lambda(\{v_i\})} e^{\mathrm{H}[\{v_i\}]-\mathrm{H}_\lambda^{RBM}[\{v_i\}]} \\ &= p_\lambda(\{h_j\}|\{v_i\}) e^{\mathrm{H}[\{v_i\}]-\mathrm{H}_\lambda^{RBM}[\{v_i\}]} \end{aligned} \tag{5.18}$$

The above Eq. (5.18) implies that when an RG transformation can be performed exactly (i.e., the variational Hamiltonian exactly equals the true Hamiltonian $\mathrm{H}[\{v_i\}] = \mathrm{H}_\lambda^{RBM}[\{v_i\}]$), T_λ is the conditional probability of a configuration of hidden spins given a configuration of visible spins. In probability theory, it would mean that the variational distribution $p_\lambda(\{v_i\})$ exactly reproduces the true distribution $P(\{v_i\})$ which makes the KL divergence $\mathrm{D}_{KL} = 0$.

5.2 Entropic Utility and Connectionism

Connectionism is a set of approaches used to study the fields of cognitive psychology, neuroscience and philosophy of mind, that models mental or behavioral phenomea as an emergent property of interconnected networks of simple computing units. The previous section established a mapping between deep learning networks based on RBMs and the variational RG procedure applied to a regular arrangement (lattice) of units (spins). In this section, we attempt to connect the notion of expected entropic utility (negative of total entropy production) Eq. (2.39) with the connectionist models (networks) which can be represented as hypercubic interacting spin-chains.

In Chapter 2, we arrived at a formalism deriving the equivalence between Entropic Utility and path diversity. This section generalizes the notion of entropy production for nonequilibrium statistical mechanics using the concept of *Massieu Functions* as presented in [Niv09]. Subsequently it is shown how the invariance of a thermodynamic Massieu function, the *Massieu-Planck potential* is related to the functional RG fixed point for a hypercubic lattice structure in the *continuum limit* (i.e., when the lattice spacing $a \to 0$) [Kop10].

5.2.1 Massieu Functions and Entropy Production

We follow the development in [Niv09]. Consider a probability distribution p_i over a properties f_r indexed by r with possible values f_{ri}. The expectation of the property f_r is given by

$$\sum_{i=1}^{s} p_i f_{ri} = \langle f_r \rangle. \tag{5.19}$$

If this expectation is only allowed to fluctuate around a mean value, the most probable (stationary) distribution of the system is given by

$$\begin{aligned} p_i^* &= \exp\Big(-\lambda_0 - \sum_{r=1}^{R} \lambda_r f_{ri}\Big) \\ &= (Z)^{-1} \exp\Big(-\sum_{r=1}^{R} \lambda_r f_{ri}\Big) \qquad (5.20) \\ Z &= \exp(\lambda_0) \\ &= \sum_{i=1}^{s} \exp\Big(-\sum_{r=1}^{R} \lambda_r f_{ri}\Big) \qquad (5.21) \end{aligned}$$

where Z is the partition function, λ_r is the r^{th} lagrange multiplier and λ_0 is the Massieu Function. The corresponding entropy is given by

$$\mathfrak{D}^* = \lambda_0 + \sum_{r=1}^{R} \lambda_r \langle f_r \rangle \tag{5.22}$$

The above derivation is generic and applies to any probabilistic system of multinomial form; it need not refer to a thermodynamic system. For a conserved property f_r, one can define the generalized heat δQ_r and generalized work δW_r as follows,

$$\begin{aligned} d\langle f_r \rangle &= \delta W_r + \delta Q_r & (5.23)\\ \delta W_r &= \sum_{i=1}^{s} p_i^* d f_{ri} & (5.24)\\ \delta Q_r &= \sum_{i=1}^{s} d p_i^* f_{ri} & (5.25) \end{aligned}$$

From Eq. (5.25) and Eq. (5.22), one gets the generalized Clausius equality

$$d\mathfrak{D}^* = \sum_{r=1}^{R} \lambda_r \delta Q_r. \tag{5.26}$$

Substituting Eq. (5.26) in the differential of the Eq. (5.22) gives

$$\begin{aligned} -d\lambda_0 &= \sum_{r=1}^{R} \lambda_r \delta W_r + \sum_{r=1}^{R} d\lambda_r \langle f_r \rangle \\ &= -d\mathfrak{D}^* + d\Big(\sum_{r=1}^{R} \lambda_r \langle f_r \rangle \Big), & (5.27) \end{aligned}$$

The Massieu function λ_0 captures all possible changes in the system due to changes in the entropy $\mathfrak{D}^*$ or in the constraint set $\{\langle f_r \rangle\}$. Consider an open system consisting of a defined region (collection of entities) in contact with some surroundings (rest of the universe). Let the internal structure of the system be described by a probability distribution p_i giving rise to an entropy function $\mathfrak{D}$ (not necessarily the thermodynamic entropy). Then a purely probabilistic formulation of the second law [Niv09] is given by

$$d\mathfrak{D}_{\text{univ}} = d\mathfrak{D}^* + \delta\mathfrak{D}_{\text{prod}} \geq 0 \tag{5.28}$$

where $\delta\mathfrak{D}_{\text{prod}}$ is the entropy exported by the system to its surroundings. The only means by which entropy can be exported to the surroundings is by reduction in magnitude of one or more constraints

$\{\langle f_r \rangle\}$ or multipliers $\{\lambda_r\}$. Thus one has

$$\delta \mathfrak{D}_{\text{prod}} = -d\Big(\sum_{r=1}^{R} \lambda_r \langle f_r \rangle\Big). \tag{5.29}$$

Using Eq. (5.29) and comparing Eq. (5.27) and Eq. (5.28) yields

$$d\lambda_0 = d\mathfrak{D}^* + \delta \mathfrak{D}_{\text{prod}} \geq 0 \tag{5.30}$$

This gives a formulation of the generalized second law for arbitrary systems described by a probability distribution under a set of constraints on its observed properties. For open thermodynamic systems, the second law is given by the entropy balance relation Eq. (2.16). Comparing Eq. (5.30) with the entropy balance relation shows that the Massieu Function is a statistical generalization of entropy production $\delta\sigma$ in open thermodynamic systems. Thus,

$$\delta\sigma \equiv \delta\lambda_0. \tag{5.31}$$

5.2.2 Functional Renormalization Group and Massieu-Planck Potential

The functional renormalization group is one of the most general and extremely powerful forms of RG devised. This technique allows one to interpolate smoothly between the known microscopic laws and the complicated macroscopic phenomena in physical systems. In this sense, it bridges the transition from simplicity of microphysics to complexity of macrophysics acting as a microscope with a variable resolution. One starts with a high-resolution picture of the known microphysical laws and subsequently decreases the resolution to obtain a coarse-grained picture of macroscopic collective phenomena. However, the real reason behind its wide acceptance in almost all disciplines of theoretical physics is its non-perturbative flow equation which does not suffer from the limitations of conventional perturbation theory, which were outlined in Chapter 4.

An energy-scale dependent form of the effective action Eq. (4.41), called effective average action, forms the basis for FRG flow equation. When the energy scale (cutoff) of the effective average action is made extremely small, the latter converges to the true effective action which describes the RG infrared fixed point. In this section, we try to derive a connection between the thermodynamic Massieu function (Massieu-Planck potential) with the exact effective action by making use of well established analogies resulting from Wick rotation from real to imaginary time Eq. (4.23).

5.2.2.1 Wetterich Flow Equation

In QFT, the dynamics of field operators are governed by the quantum equation of motion obtained by variation of the effective action Υ with the vacuum expectation value of the fields $\bar{\Phi}$ as.

$$\frac{\delta}{\delta\bar{\Phi}}\Upsilon[\bar{\Phi}] = J, \tag{5.32}$$

where J is a source field. In most cases of interest, it is not possible to evaluate the exact effective action directly. A versatile approach to the computation of the effective action is based on Wilsonian RG described in Chapter 3. In FRG, one constructs an interpolating action Υ_k, also called the effective average action, with a momentum shell parameter k such that Υ_k corresponds to the bare classical action S_{bare} to be quantized, for some large ultraviolet scale $k \to \Lambda$. The requirement is that full quantum effective action Υ should be recovered from the average action as $k \to 0$. The dependence of effective average action on the scale k is obtained by adding an IR regulator term ΔS_k to the bare action in the generating functional Eq. (4.19) to yield

$$Z_k[J] = \int_\Lambda \mathscr{D}\Phi e^{-S[\Phi]-\Delta S_k[\Phi]+\int J\Phi} \tag{5.33}$$

where

$$\Delta S_k[\Phi] = \frac{1}{2}\int \frac{d^D q}{(2\pi)^D}\Phi(-q)R_k(q)\Phi(q) \tag{5.34}$$

is an IR regulator that can be viewed as a momentum k dependent mass term as it is quadratic in Φ. The regulator function $R_k(q)$ should satisfy certain conditions in order to meet the requirements for the effective average action. These conditions are

$$\lim_{q^2/k^2\to 0} R_k(q) > 0 \tag{5.35}$$

$$\lim_{k^2/q^2\to 0} R_k(q) = 0 \tag{5.36}$$

$$\lim_{k^2\to\Lambda\to\infty} R_k(q) \to \infty \tag{5.37}$$

The condition Eq. (5.35) implies the IR regularization (i.e., screens out the IR modes $q^2 \ll k^2$). The condition Eq. (5.36) implies that regulator vanishes for $k \to 0$. As a consequence, one recovers the generating functional and full quantum effective action in this limit. The condition Eq. (5.37) allows to associate the classical bare action S_{bare} with the effective average action at the ultraviolet scale Λ. Since we have already established that the interpolating action Υ_k exhibits the correct limits, we can study its trajectory through the theory space. Using the DeWitt notation, we have the scale

dependent generating functional $Z_k[J]$ as

$$\exp(W_k[J]) = Z_k[J] = \int \mathscr{D}\Phi \exp\Big(-S[\Phi] - \frac{1}{2}\Phi R_k \Phi + J\Phi \Big) \tag{5.38}$$

where J is the source field. The VeV of the field operator is then given by

$$\bar{\Phi}[J;k] = \frac{\delta W_k}{\delta J}[J]. \tag{5.39}$$

This can be inverted to give $J_k[\bar{\Phi}]$. The Legendre transform of W_k, after subtracting out the regulator, gives the effective average action as

$$\Upsilon_k[\bar{\Phi}] = \Big(-W_k\big[J_k[\bar{\Phi}]\big] + J_k[\bar{\Phi}]\bar{\Phi} \Big) - \frac{1}{2}\bar{\Phi} R_k \bar{\Phi} \tag{5.40}$$

As the regulator R_k is the only term explicitly dependent on the scale k, on differentiating the effective average action with respect to k one gets the Wetterich flow equation (also the FRG flow equation)

$$\frac{d}{dk}\Upsilon_k[\bar{\Phi}] = \frac{1}{2}\mathrm{Tr}\left[\left(\frac{\delta^2 \Upsilon_k}{\delta\bar{\Phi}\delta\bar{\Phi}} \right)^{-1} \frac{d}{dk} R_k \right] \tag{5.41}$$

As the IR regulator R_k is arbitrary besides satisfying the conditions Eq. (5.35) to Eq. (5.37), there are infinitely many interpolating actions Υ_k. At the infrared scale $k \to 0$ however, the full effective action $\Upsilon_{k=0} = \Upsilon$ is recovered for every choice of regulator R_k and all trajectories meet at the same point in theory space spanned by the running couplings.

5.2.2.2 Effective Action and Massieu-Planck Potential

Consider a function of energy-scale $\tilde{F}(k)$ and its fourier transform in time as $F(t)$ (as energy-scale is the fourier-conjugate of time in Minkowski space). Then we have

$$\tilde{F}(k) = \int_0^\infty F(t) e^{-ikt}\, dt, \tag{5.42}$$

Using Wick rotation to rotate the function $F(t)$ in real time to $F(\tau)$ in imaginary time, we have

$$\tilde{F}(k) = -i \int_0^\beta F(\tau) e^{-k\tau}\, d\tau \tag{5.43}$$

where β is the inverse temperature. Similarly one has

$$\begin{aligned} k\tilde{F}(k) &= -i\int_0^\infty \frac{d}{dt}F(t)e^{-ikt}\,dt \\ &= -i\int_0^\beta \frac{d}{d\tau}F(\tau)e^{-k\tau}\,d\tau. \end{aligned} \tag{5.44}$$

Integrating Eq. (5.44) by parts,

$$k\tilde{F}(k) = -i\Big(F(\beta)e^{-k\beta} - F(0)\Big) - ik\int_0^\beta F(\tau)e^{-k\tau}\,d\tau. \tag{5.45}$$

Using Eq. (5.43) in Eq. (5.45), we have

$$k = \frac{1}{\beta}\log\left(\frac{F(\beta)}{F(0)}\right), \tag{5.46}$$

This expression Eq. (5.46) allows us to define the energy-scale k in terms of the inverse temperature β. Furthermore,

$$k \to 0 \quad \Longrightarrow \quad \beta \to \infty \quad \textbf{OR} \quad F(\beta) = F(0) \tag{5.47}$$

Wick rotation relates statistical mechanics in d+1 dimensions with field theory in (d,1) dimensions. The role of the generating functional $Z[J]$ in field theory is played by the partition function $Z(\beta)$ in thermodynamics [Kop10]. The Legendre transformation of $\log\big(Z[J]\big)$ with respect to VeV of the order parameter field $\bar{\Phi}$ gives the Effective Action $\Upsilon[\bar{\Phi}]$. Similarly, Legendre transformation of $\log\big(Z(\beta)\big)$ with respect to volume V (or any generalized displacement) yields the negative of Massieu-Planck potential (or Gibbs free entropy) $\lambda_0(\beta)$. Mathematically,

$$\begin{aligned} -\lambda_0(\beta) &= \beta PV - \log\big(Z(\beta)\big) \\ &= \beta PV + \beta F \\ &= \beta G \end{aligned} \tag{5.48}$$

where P is the pressure (or the generalized force conjugate to the generalized displacement V), F is the Helmholtz free energy and G is the Gibbs Free Energy. As the name suggests, Massieu-Planck potential is just a Massieu function in the thermodynamic limit. Thus, effective action in field theory $\Upsilon[\bar{\Phi}]$ is related to the Massieu-Planck potential $\lambda_0(\beta)$ in thermodynamics via Wick rotation. Formally,

using Eqs. (5.47), (5.36) and neglecting the trivial case $\beta \to \infty$, we have

$$\Upsilon[\bar{\Phi}] = \lim_{k\to 0} \Upsilon_k[\bar{\Phi}] = \lim_{k\to 0}\left(\Upsilon_k[\bar{\Phi}] + \frac{1}{2}\bar{\Phi}R_k\bar{\Phi}\right) \tag{5.49}$$

and

$$\lambda_0(\beta) = \lambda_0(0) \quad \Longrightarrow \quad \delta\lambda_0 = 0 \tag{5.50}$$

The above relations state that the exact effective action $\Upsilon[\bar{\Phi}]$ describing the RG fixed point of a continuum lattice keeps the macroscopic Massieu-Planck potential $\lambda_0(\beta)$ invariant. Then from Eq. (5.31), we infer that the entropy production $\delta\sigma = 0$ at the RG fixed point. The expected entropic utility Eq. (2.39) therefore attains its maximum value of 0 at the RG fixed point (as $\delta\sigma \geq 0$ from the second law).

CHAPTER

6

EPILOGUE

6.1 Outcomes

There are two major outcomes of this work. The first major outcome is a connection between decision theoretic rationality and causal entropic forces. The theory of causal entropic forces is based on the idea of maximizing causal path entropy by evaluating path probabilities up to a finite time horizon instead of greedily maximizing the instantaneous entropy production. However, adhering to classical thermodynamics, one cannot fully explain the origins of such a path based force acting on a macrostate of a classical ensemble. We establish how such a force might originate in the quantum mechanical framework for projective interactions. This is subsequently extended to general (nonprojective) interactions by coming up with a formulation of path diversity in terms of the maximum system entropy that cane be reached from the present time to a future time horizon for a fixed exchange of heat with the surroundings. Using this formulation, it is shown how maximizing future path diversity amounts to minimizing the total entropy production of the system and bath composite. Using the Hamiltonian theory of dynamic economics, it is shown how negative of the entropy production takes the form of the Bellman Equation where the expectation of the utility measure over the ensemble is shown to be proportional to negative Kullback-Liebler divergence between the current distribution and the stationary state.

The second major outcome is to show how maximizing path diversity in the context presented

above in a network of connected units can lead to behaviors typical of thermodynamic systems at the critical point of phase transition. Power law scaling is a characteristic of physical systems at their continuous phase transition point. There is a huge volume of literature published on empirical studies of neuronal activity in the human brain which show a power law behavior, although the mechanisms behind such behaviors remain unexplained so far. Using Wick rotation, we show how the non-trivial fixed point (critical point) of the functional renormalization group flow equation maps to minimization of the change in the thermodynamic Massieu function (the Massieu-Planck potential), which is a statistical generalization of entropy production for nonequilibrium dynamics. It therefore provides an explanation of critical organization of a connected network of interacting units which try to maximize this expected discounted utility sum (i.e., the negative of entropy production) which is tantamount to maximizing path diversity in the context of causal entropic forces.

6.2 Future Work

One of the open questions in cognitive neuroscience is what constitutes human knowledge and how it is efficiently stored and represented in the brain. It would be interesting to see if the notion of entropic utility developed in this work provides some insight in the area. Giulio Tononi, in his paper on integrated information and consciousness [Ton08], proposes that consciousness can be termed as the collective (or integrated information) procured using all of the parts of the system as against the sum of information procured using each individual part. Just like the expected utility measure Eq. (2.40), Tononi also uses the KL divergence between the actual (a posteriori) and potential (a priori) repertoires of system states to quantify integrated information and subsequently consciousness. It would be worthwhile to investigate this connect further in future.

As for Artificial Intelligence research, it would be of great interest to the planning community to see if it is possible to identify the classical notion of goals, widely used in conventional AI paradigms, with maximizing future path diversity (or future freedom of action) in connectionist architectures.

BIBLIOGRAPHY

[Arr50] Arrow, K. J. "A Difficulty in the Concept of Social Welfare". *Journal of Political Economy* **58**.4 (1950), pp. 328–346.

[Bac] Baccarin, S. "Optimal Consumption of a generalized Geometric Brownian Motion with Fixed and Variable Intervention Costs".

[BS50] Baez, J. C. & Stay, M. "Algorithmic Thermodynamics". *arXiv:1010.2067 [math-ph]* (1950).

[BP02] Breur, H. P. & Petruccione, F. *The Theory of Open Quantum Systems*. Oxford University Press, New York, 2002.

[CS76] Cass, D. & Shell, K. *The Hamiltonian Approach to Dynamic Economics*. Academic Press Inc., 1976.

[Kit09] Kitzbichler, M. G. et al. "Broadband Criticality of Human Brain Network Synchronization". *PLOS Computational Biology* **5**.3 (2009).

[Kop10] Kopietz, P. et al. *Introduction to the Functional Renormalization Group*. Vol. 798. Lecture Notes in Physics. Springer-Verlag, Berlin, 2010.

[McC04] McComb, W. D. *Renormalization Methods: A guide for beginners*. Clarendon Press, 2004.

[MS14] Mehta, P. & Schwab, D. J. "An exact mapping between the Variational Renormalization Group and Deep Learning". *arXiv:1410.3831v1 [stat.ML]* (2014).

[Niv09] Niven, R. K. "Minimization of a free-energy-like potential for non-equilibrium flow systems at steady state". *Philosophical Transactions of the Royal Society B: Biological Sciences* **365**.1545 (2009), pp. 1323–1331.

[Sha14] Shah, S. "Quantum Mechanical Foundations of Causal Entropic Forces". *Artificial General Intelligence: Proceedings of the Seventh International Conference (AGI 2014)*. Vol. 8598. Lecture Notes in Computer Science. Springer International Publishing, Switzerland, 2014, pp. 165–193.

[Ste93] Sterman, G. *An Introduction to Quantum Field Theory*. Cambridge University Press, 1993.

[Ton08] Tononi, G. "Consciousness as Integrated Information: a Provisional Manifesto". *The Biological Bulletin* **215** (2008), pp. 216–242.

[WGF13] Wissner-Gross, A. D. & Freer, C. E. "Causal Entropic Forces". *Physical Review Letters* **110**.168702 (2013), pp. 1–5.